Continental Shelf Research 31 (2011) 340–355

Contents lists available at ScienceDirect

Continental Shelf Research

journal homepage: www.elsevier.com/locate/csr

Research papers

Latitudinal patterns of export production recorded in surface sediments of the Chilean Patagonian fjords (41–55°S) as a response to water column productivity

Claudia Aracena [a,*], Carina B. Lange [b,c], José Luis Iriarte [c,d], Lorena Rebolledo [e], Silvio Pantoja [b,c]

[a] Programa de Postgrado en Oceanografía, Departamento de Oceanografía, Universidad de Concepción, Casilla 160-C, Concepción, Chile
[b] Departamento de Oceanografía and Centro de Investigación Oceanográfica en el Pacífico Sur-Oriental (COPAS), Universidad de Concepción, Casilla 160-C, Concepción, Chile
[c] Programa COPAS Sur-Austral, Universidad de Concepción, Casilla 160-C, Concepción, Chile
[d] Instituto de Acuicultura, Universidad Austral de Chile, Casilla 1327, Puerto Montt, Chile
[e] Instituto de Biología Marina, Facultad de Ciencias, Universidad Austral de Chile, Casilla 567, Valdivia, Chile

ARTICLE INFO

Article history:
Received 23 November 2009
Received in revised form
9 August 2010
Accepted 18 August 2010

Keywords:
Biogenic opal
Organic carbon
Stable carbon isotopes
Primary production
Fjords
Patagonia

ABSTRACT

The Chilean Patagonian fjords region (41–56°S) is characterized by highly complex geomorphology and hydrographic conditions, and strong seasonal and latitudinal patterns in precipitation, freshwater discharge, glacier coverage, and light regime; all of these directly affect biological production in the water column. In this study, we compiled published and new information on water column properties (primary production, nutrients) and surface sediment characteristics (biogenic opal, organic carbon, molar C/N, bulk sedimentary $\delta^{13}C_{org}$) from the Chilean Patagonian fjords between 41°S and 55°S, describing herein the latitudinal pattern of water column productivity and its imprint in the underlying sediments. Based on information collected at 188 water column and 118 sediment sampling sites, we grouped the Chilean fjords into four main zones: Inner Sea of Chiloé (41° to ~44°S), Northern Patagonia (44° to ~47°S), Central Patagonia (48–51°S), and Southern Patagonia (Magellan Strait region between 52° and 55°S). Primary production in the Chilean Patagonian fjords was the highest in spring–summer, reflecting the seasonal pattern of water column productivity. A clear north–south latitudinal pattern in primary production was observed, with the highest average spring and summer estimates in the Inner Sea of Chiloé (2427 and 5860 mg C m^{-2} d^{-1}) and Northern Patagonia (1667 and 2616 mg C m^{-2} d^{-1}). This pattern was closely related to the higher availability of nutrients, greater solar radiation, and extended photoperiod during the productive season in these two zones. The lowest spring value was found in Caleta Tortel, Central Patagonia (91 mg C m^{-2} d^{-1}), a site heavily influenced by glacier meltwater and river discharge loaded with glacial sediments. Biogenic opal, an important constituent of the Chilean fjord surface sediments (Si_{OPAL} ~1–13%), reproduced the general north–south pattern of primary production and was directly related to water column silicic acid concentrations. Surface sediments were also rich in organic carbon content and the highest values corresponded to locations far away from glacier influence, sites within fjords, and/or semi-enclosed and protected basins, reflecting both autochthonous (water column productivity) and allochthonous sources (contribution of terrestrial organic matter from fluvial input to the fjords). A gradient was observed from the more oceanic sites to the fjord heads (west–east) in terms of bulk sedimentary $\delta^{13}C_{org}$ and C/N ratios; the more depleted ($\delta^{13}C_{org}$ −26‰) and higher C/N (23) values corresponded to areas close to rivers and glaciers. A comparison of the Chilean Patagonian fjords with other fjord systems in the world revealed high variability in primary production for all fjord systems as well as similar surface sediment geochemistry due to the mixing of marine and terrestrial organic carbon.

1. Introduction

The Chilean Patagonian fjords region, located between 41° and 56°S, cover roughly 241,000 km^2, an area characterized by an extensive coastline composed of a large number of islands, fjords, sounds, and gulfs that were formed by glacial erosion during the Quaternary and tectonic sinking of the central Chilean valley (Borgel, 1970; Rabassa, 2008). The complex topography limits or controls the exchange of waters between coastal regions and the open ocean, creating micro-environments with oceanographic conditions that sustain unique ecosystems. These are characterized by complex marine–terrestrial–atmospheric interactions that

* Corresponding author. Tel.: +56 41 220 3557; fax: +56 41 220 7254.
E-mail address: claudiaaracena@udec.cl (C. Aracena).

0278-4343/$ - see front matter
doi:10.1016/j.csr.2010.08.008

result in high biological production. Strong seasonal climatic changes (e.g., solar radiation, wind, precipitation) as well as different physical regimens (mixing and/or stability of the water column) impose an external influence on the phytoplankton, which displays seasonal changes in biomass, primary production, and species composition (e.g., Saggiomo et al., 1994; Pizarro et al., 2000; Iriarte et al., 2007).

At present, Patagonia has three main glacial systems: the Northern Patagonian Icefield (46–47°S), Southern Patagonian Icefield (48–52°S), and the Darwin Mountains Icefield in Tierra del Fuego (54–55°S). The inventoried glaciers in Patagonia total 16,159 km^2, of which the Northern and Southern Patagonian Icefields contribute 4200 and 9659 km^2, respectively (Rivera et al., 2002) and the Darwin Icefield ~2300 km^2 (Lliboutry, 1998). The Patagonian Icefields are dominated by calving glaciers that release icebergs and introduce clay and freshwater plumes into the fjord heads. The main continental freshwater sources, however, are several rivers that discharge into the fjords. Averaged gauged river flows of the principal rivers are: Baker (1133 $m^3 s^{-1}$), Pascua (753 $m^3 s^{-1}$), and Bravo (112 $m^3 s^{-1}$) in Central Patagonia; Aysén (283 $m^3 s^{-1}$) and Cisnes (253 $m^3 s^{-1}$) in Northern Patagonia; Puelo (678 $m^3 s^{-1}$) and Petrohué (278 $m^3 s^{-1}$), which discharge into the Reloncaví fjord; and Yelcho (363 $m^3 s^{-1}$), which flows into the Corcovado Gulf (Dirección General de Aguas, www.dga.cl).

The terrestrial organic matter in the inlets originates from the surrounding evergreen rainforest (e.g., Villagrán, 1988). The vegetation distribution is controlled latitudinally and altitudinally by sharp temperature and precipitation gradients (Abarzúa et al., 2004, and references therein). The anthropogenic input of organic matter is largely confined to the region's main cities: Puerto Montt, Castro, Coyahique, Puerto Aysén, and Punta Arenas. However, population density is very low in Patagonia, which is one of Chile's least populated regions (Instituto Nacional de Estadística, http://www.ine.cl).

Intense use of the area began in the 1980s with activities related to aquaculture, fisheries, tourism, and human settlements. Aquaculture is one of the activities that has experienced the largest growth and development in the last decade, especially in Regions X (De los Lagos, 39°15′–44°04′S) and XI (Aysén, 43°38′–49°16′S). Salmon-cage farming is one of the most important export commodities of the country.

Most of the oceanographic information for the Chilean fjords and channels (from Puerto Montt at 42°S to Cape Horn at 56°S) comes from the CIMAR Program (Cruceros de Investigación Marina en Áreas Remotas; Marine Research Cruises in Remote Areas). This is an ongoing program of the Comité Oceanográfico Nacional (CONA; National Oceanographic Committee) that started with its first cruise in 1995. During all CIMAR cruises, the water column and surface sediments were sampled intensively and, on some occasions, sediment cores were also collected. This yielded a large database of physical (temperature, salinity, light penetration, currents, tides), chemical (dissolved oxygen, nutrients), and biological (phytoplankton, chlorophyll-*a*, zooplankton, red tides) characteristics of the water column along with a characterization of the sediments in terms of grain size, porosity, carbon, nitrogen, trace metals, stable and radioactive isotopes, and organic components (see Silva and Palma (2008) for the history of the CIMAR Program).

In this study we compiled published and new information on water column properties (primary production, nutrients) and surface sediment characteristics (biogenic opal, organic carbon, molar C/N, bulk sedimentary $\delta^{13}C_{org}$) in the Chilean fjord region, describing the latitudinal pattern (41–55°S) of water column productivity and its imprint in the underlying sediments. We use the contents of biogenic opal and organic carbon in the sediments as proxies of export production, and the molar C/N and stable carbon isotope signature for tracing the sources of organic matter in this coastal sedimentary environment. We discuss the observed sediment patterns in relation to latitudinal differences in precipitation, river discharges, and glacier coverage. Finally, we compare the Chilean fjords to other fjord systems in the world.

2. Study area

2.1. Climate

The southeast Pacific and southern Chile (south of 40°S) are strongly influenced by the Southern Westerly Winds (SWW). These, in turn, are affected by the strength of the Subtropical Pacific Anticyclone and the position of the Antarctic Convergence, resulting in strong latitudinal temperature and precipitation gradients (Strub et al., 1998). There is a marked contrast between the maritime climate of the western coastal ranges and the dry climate of the Argentinean plains of eastern Patagonia. Miller (1976) sub-divides southern Chile at 42°S, with a cool temperate band to the south and a warm temperate band to the north of this latitude. The southern band comprises prevailing SWW year-round, with little seasonality. The north–south pressure gradient, the SWW, and precipitation are at a maximum around 50°S, with over 300 days of rainfall in some places and mean annual cloud cover of more than 0.85 tenths (Kerr and Sudgen, 1994).

Precipitation in the Chilean Patagonian fjords region ranges from 1000 to 7000 mm yr^{-1} on the western side of the Andes (Fig. 1). Conversely, the eastern side of the Andes receives less rainfall (300–700 mm yr^{-1}), with Tierra del Fuego recorded as the driest region (380 mm in Punta Arenas at 53°08′ S) (Dirección General de Aguas Chile, www.ine.cl; GeoClima, www.dgf.uchile.cl/geoclima). The annual temperature range is typically small for a

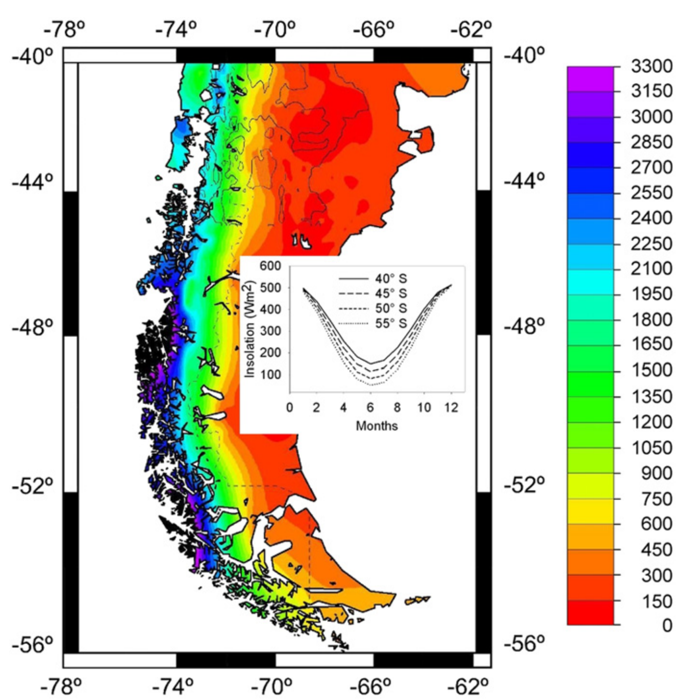

Fig. 1. Precipitation map for Patagonia. The vertical color bar represents the average annual precipitation for the period 1960–1991; information taken from New et al. (2002). The inset figure represents average monthly insolation values (W m^{-2}) for every 5° latitude between 40° and 55°S for the year 2004 as an example (http://aom.giss.nasa.gov/srmonlat.html).

maritime climate and the mean temperature oscillates between 5.5 °C in the extreme south (54°S) and 11 °C at 42°S (Miller, 1976).

Insolation has a marked latitudinal and seasonal pattern. Annual mean values are the highest at 40°S and the lowest at 55°S ($W\,m^{-2}$, Atmosphere–Ocean Model, http://aom.giss.nasa.gov/srmonlat.html). On a seasonal scale, insolation values are higher in austral spring–summer (October–January) than in winter (June–August) (Fig. 1, inset).

2.2. Oceanography

The southern Pacific coast of the South American continent is under the oceanic influence of the West Wind Drift Current, which divides into two branches upon reaching the Chilean coast, transporting sub-Antarctic water along the coast. The northern branch is known as the Humboldt or Peru–Chile Current and the southern branch as the Cape Horn Current (Silva and Neshyba, 1979). Driven by the West Wind Drift, sub-Antarctic water penetrates the inlets (Silva et al., 1998).

The three main glacial fields and especially several major rivers mentioned above incorporate fresh waters into the fjord system, inducing estuarine conditions with a stratified two-layer water column (Silva et al., 1995), with net movement in the surface layer towards the adjacent ocean and in the deep layer towards the fjords. This onshore flow delivers oceanic nutrients to the nearshore region below the surface waters (sub-Antarctic Water, loaded with macronutrients). The upper 20–30 m of the water column have very low salinity and are usually devoid of nutrients other than dissolved silicon derived from river runoff (Silva and Neshyba, 1979; Iriarte et al., 2007); this surface layer deepens offshore (Pickard, 1971; Strub et al., 1998; Dávila et al., 2002). Strong vertical gradients (pycnocline, oxycline, nutricline) separate the upper layer from the deep layer (Sievers and Silva, 2008), and mixing is necessary to bring nutrients up into the euphotic zone (Montecino et al., 2004). The interaction between sub-Antarctic waters and the diluted waters from the fjords define a coastal salinity front between 42° and 56°S (Silva and Neshyba, 1979; Dávila et al., 2002). The front is present during the whole year, with the strongest gradients in summer (Acha et al., 2004). Details on the water masses in the Chilean fjord region and schematic models of general circulation patterns can be found in Sievers and Silva (2008).

It is important to remark that circulation and water mass exchange between basins is limited by important submarine topographical features (i.e., Desertores, Meninea, Angostura Inglesa, and Carlos III constrictions). These impose important contrasts among the four oceanographic zones in terms of organic matter production due to differences in nutrient availability (Sievers and Silva, 2008).

2.3. Plankton

Published information on chlorophyll-*a* and primary productivity show that the fjord area between 41° and 56° S is highly variable. Values reported for the Inner Sea of Chiloé and the head of the fjords (41–43°S) range from 1–25 mg Chl-*a* m^{-3} and 1–23 mg C $m^{-3}\,h^{-1}$, respectively (Iriarte et al., 2007); further south, values for the area between Penas Gulf and the Magellan Strait (47–50° S) range from 0.1–15 mg Chl-*a* m^{-3} to 1.5–96 mg C $m^{-3}\,h^{-1}$, respectively (Pizarro et al., 2000).

Phytoplankton assemblages show high spatial and temporal heterogeneity (Alves-de-Souza et al., 2008, and references therein). Diatoms are the most frequent and abundant group year-round (predominance of R-strategist species), whereas dinoflagellates are only important on some occasions (when they form blooms), and nanoflagellate abundances are highest in summer and autumn in the most southern area. Paredes and Montecino (this issue) show that the dominant size fraction depends on total chlorophyll-*a*: small phytoplankton cells dominate in winter or at stations with continental influence when total chlorophyll-*a* values are low, whereas the larger micro-phytoplankton fraction prevails in spring when total chlorophyll-*a* values are high.

The high rates of phytoplankton growth in spring–summer (Avaria et al., 1999; Pizarro et al., 2000) favor the abundance of planktonic herbivores and carnivores (e.g., Palma and Silva, 2004). Planktonic crustaceans (copepods, euphausiids) are the most abundant in the fjords and channels, followed by chaetognaths and gelatinous carnivores (Palma and Silva, 2004). A recent study on the fate of primary production in the pelagic food web of the Inner Sea of Chiloé (González et al., 2010) reveals contrasting grazing pressure of zooplankton and export production for spring and winter: zooplankton grazing on diatom-dominated microplankton and the relative dominance of the classical food web with increased export production *vs*. zooplankton grazing on nanoplankton and the relative dominance of the microbial loop with lower export production, respectively.

2.4. Sediments

Silva and Prego (2002) spatially segregate the whole Patagonian Region into three large macro-zones (each having several sub-zones) according to the distribution of the carbon and nitrogen concentrations in the sediments: Northern (Puerto Montt to Península Taitao), Central (Golfo de Penas to Strait of Magellan), and Southern (Magellan to Cape Horn) zones. These macro-zone have mean organic carbon values of 0.38–1.75% (Northern Zone), 0.44–1.43% (Central Zone), and 0.29–0.90% (Southern Zone) (see Silva, 2008). In general, the terrigenous organic matter content in the sediments increases from the oceanic area to the heads of the fjords due to local river discharges (Pinto and Bonert, 2005). Sediments influenced by glaciers have very low organic matter due to dilution by the large amounts of inorganic matter contributed by glaciers (Silva, 2008, and references therein). Based on carbon:nitrogen ratios, Silva and Prego (2002) observe values between 5.4 and 11.4 (for the entire Patagonia fjords area), and Sepúlveda et al. (this issue) reports ratios of 9.6–16.9 (in fjords from Northern Patagonia). Both works show that this ratio increases from the open ocean sediments to inner fjord areas.

Sedimentation rates are high in the Chilean fjords. Estimated values based on ^{210}Pb are 0.26–0.36 cm yr^{-1} for Aysén Fjord and Costa Channel (Rojas, 2002; Salamanca and Jara, 2003); 0.15 cm yr^{-1} for Cupquelán Fjord, 0.67 cm yr^{-1} for Quitralco Fjord (Salamanca and Jara, 2003); and 0.25–0.75 cm yr^{-1} for Puyuhuapi Channel (Rebolledo et al., 2005; Sepúlveda et al., 2005). For the oceanic area off Chiloé and the western entrance of the Magellan Strait, estimated sedimentation rates are 0.22–0.29 cm yr^{-1} (Muñoz et al., 2004) and 0.25 cm yr^{-1} (Muñoz, pers. comm.), respectively.

During the *CIMAR 7* Fiordos cruise, sediment cores encompassing the last 2000 years of sedimentation were retrieved from Northern Patagonia. The study of these records reveals periods of variable marine and continental contributions, temperature, and humidity intimately linked to SWW intensity at interdecadal/multi-decadal scales (e.g., Rebolledo et al. 2008; Sepúlveda et al., 2009). Recent works on marine and lake sediments from Northern Patagonia and the adjacent oceanic area also demonstrate that fluctuations in El Niño Southern Oscillation (ENSO) activity and associated low-latitude climate systems have a strong control over the climatic variability of this region (e.g., Ariztegui et al., 2007; Mohtadi et al., 2007; Rebolledo et al., 2008).

In the past six years, several international cruises have taken place in the Chilean fjords and adjacent oceanic area. These cruises, which aimed to recover high-resolution long sediment cores encompassing the time period since the Last Glacial Maximum, were: *JAMSTEC Beagle* expedition 2003, *Palmer* cruise *NBP0505* 2005, *PACHIDERME* cruise 2007, and *Mirai MR08-06* leg 2 in 2009, which also included present-day observations of water column chemistry and biology as well as pelagic–benthic coupling.

3. Material and methods

Our study area covered 14° of latitude (41–55°S) and included water column and surface sediment data (see below). The diversity of the Chilean fjord system in terms of sedimentary environment was mainly derived from its geomorphology, rainfall type and patterns, glacier coverage, and productivity related to nutrient and light availability. Given this heterogeneity and based on the initial spatial segregation defined by Silva and Prego (2002), we grouped the Chilean fjords into four main zones: (1) Inner Sea of Chiloé, from Reloncaví Fjord (41°S) to the Guafo Mouth (~44°S); (2) Northern Patagonia, from the north entrance of Moraleda Channel to Cupquelán Fjord, also including oceanic sites (44°–~47°S); (3) Central Patagonia, from ~48°S to Concepción Channel (51°S); and (4) Southern Patagonia, which includes the Magellan Strait region between ~52°S and Marinelli Fjord (~55°S) (Fig. 2).

In order to summarize and characterize each fjord, sound, and/or channel system, water column and sediment data were averaged first by location (using all stations within each location) and then locations were averaged by zone in order to describe a general zonal productivity pattern and its imprint in the sediments of the Chilean fjords. All locations in tables and figures are organized from north to south.

3.1. Water column data

Primary production (PP) and/or nutrient concentration data were available for a total of 188 water column stations. This information was summarized by location within each zone (Table 1), as mentioned above, in order to give an overview of the patterns of PP and nutrients in spring (and summer when available) in the four zones of Patagonia. The Inner Sea of Chiloé was represented by 49 water column stations, whereas Northern, Central, and Southern Patagonia were composed of 101, 17, and 21 water column stations, respectively.

Published data was obtained from the CENDHOC reports (Centro Nacional de Datos Hidrográficos y Oceanográficos de Chile) for the spring legs of the *CIMAR* cruises *8*, *9*, and *10* (Inner Sea of Chiloé); *4*, *7*, *8*, and *9* (Northern Patagonia); *2* (Central Patagonia); and *3* (Southern Patagonia) carried out in the Chilean fjord region between 1995 and 2004 onboard the *AGOR Vidal Gormáz* (http://www.shoa.cl/cendhoc/organizacion/datareport_cimar.htm). In addition, we included new unpublished information from the more recent spring *CIMAR* cruises: *12* (Inner Sea of Chiloé), *13* (Northern Patagonia), and *14* (Central Patagonia) carried out in 2006, 2007, and 2008, respectively. For the new PP estimates, water samples were collected at depths of 0, 5, 15, and 30 m using 5-L PVC Go-Flo bottles. The retrieved samples were incubated in 125-mL borosilicate polycarbonate bottles (two clear+one dark bottle) and placed in a natural-light incubator for ca. 4 h (mainly between 10:00 AM and 14:00 PM). Temperature was regulated by running surface seawater over the incubation

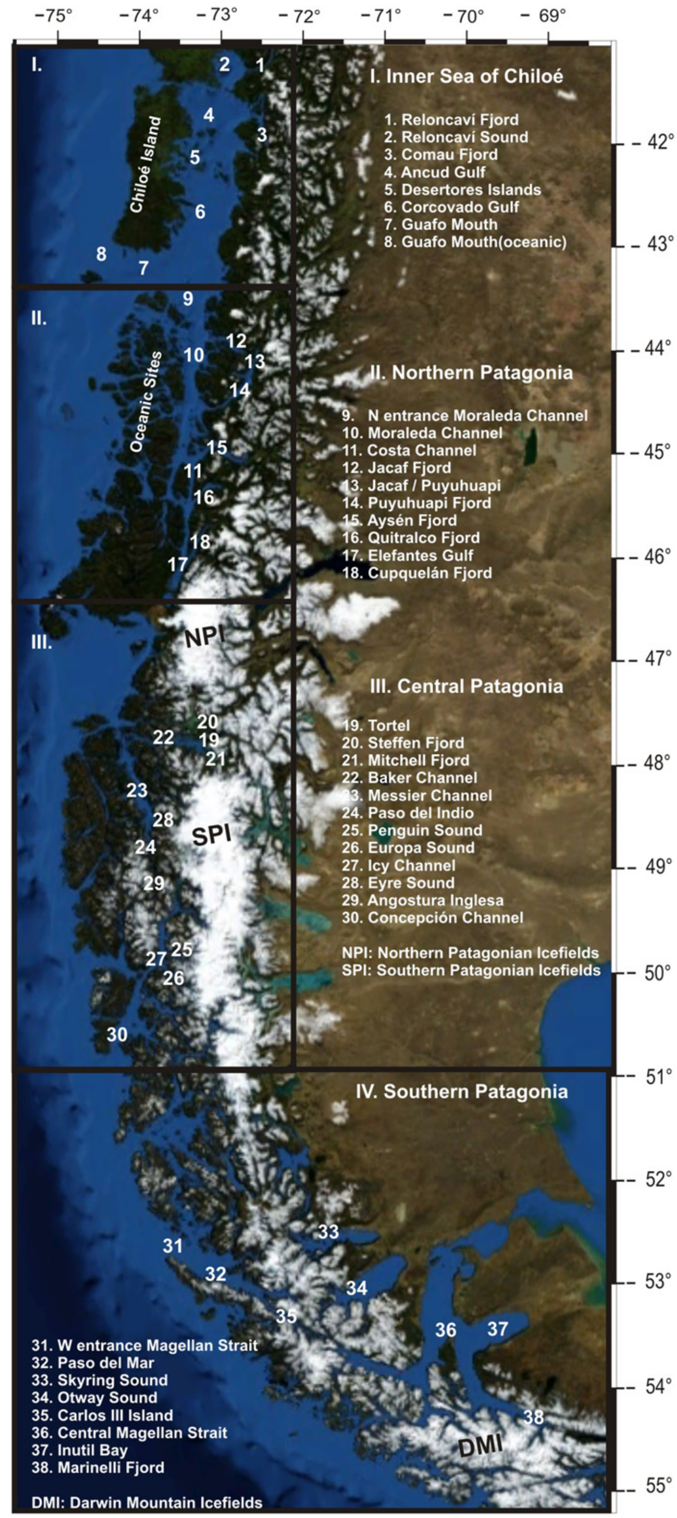

Fig. 2. Map of the Chilean Patagonia (NASA World Wind 1.4) and the locations studied in each of the four zones, from N to S: Inner Sea of Chiloé; Northern, Central, and Southern Patagonia.

bottles. Sodium bicarbonate (20–40 μCi–$NaH^{14}CO3$) was added to each bottle. Primary production was measured using the method described by Steemann-Nielsen (1952). Samples were manipulated under subdued light conditions during pre- and post-incubation periods. Filters (0.7 μm) were placed in 20-mL plastic scintillation vials and kept at −15 °C until reading (15 days later).

Table 1
Water column. Averaged primary production and nutrient concentrations for each location within each of the four zones: Inner Sea of Chiloé; Northern, Central, and Southern Patagonia. Blank spaces = no data.

Zone	Location	No. of stations	PP (mg C m^{-2} d^{-1})		Nutrients in spring		
			Spring	Summer	NO_3^- (μM)	PO_4^{-3} (μM)	$Si(OH)_4$ (μM)
Inner Sea of Chiloé	Reloncaví Fjord	8	4754.41	9406.84	5.48	0.85	23.81
	Reloncaví Sound	4			8.38	1.14	9.02
	Comau Fjord	4	1147.83	2313.50	5.02	0.79	7.13
	Ancud Gulf	18			5.97	1.17	3.74
	Corcovado Gulf	6	2228.41		12.04	1.57	5.58
	Guafo Mouth	4	134.10		6.11	0.96	3.42
	Guafo Mouth (oceanic)	5	3875.13		4.32	0.70	2.25
Northern Patagonia	N entrance Moraleda Channel	5	4812.64		7.81	0.91	6.75
	Moraleda Channel	25	3504.43	2687.30	7.70	0.89	9.53
	Costa Channel	2		1424.00	11.50	1.30	27.25
	Jacaf Fjord	4	235.80		4.50	0.69	7.29
	Jacaf/Puyuhuapi	1	289.80		2.36	0.47	9.60
	Puyuhuapi Fjord	6	869.49	1975.14	2.43	0.47	13.28
	Aysén Fjord	20	540.55	4381.00	9.29	0.95	34.03
	Quitralco Fjord	5	2295.00		11.40	1.23	14.95
	Elefantes Gulf	6	793.58		10.67	1.17	24.75
	Cupquelán Fjord	1			7.58	0.87	
	Oceanic Sites	26			6.37	0.90	5.81
Central Patagonia	Tortel	1	91.00		2.03	0.31	19.50
	Steffen Fjord	2	345.29				
	Baker Channel	2			1.57	0.38	6.50
	Messier Channel	4	463.16		4.20	0.47	1.75
	Paso del Indio	1	994.50				
	Penguin Sound	1			0.30	1.52	4.00
	Europa Sound	1			3.60	0.67	2.00
	Eyre Sound	1	799.00		7.28	0.52	2.75
	Icy Channel	1	1093.50		3.85	0.79	1.25
	Concepción Channel	3	977.58		5.64	0.97	1.00
Southern Patagonia	W entrance Magellan Strait	3		344.61	5.70	0.78	6.88
	Paso del Mar	5	106.00	407.43	5.64	0.78	7.25
	Otway Sound	1	1704.00				
	Carlos III Island	3		238.64	5.83	0.75	2.50
	Central Magellan Strait	7	1741.67	681.48	5.19	0.80	4.38
	Inutil Bay	1			5.28	0.77	3.33
	Marinelli Fjord	1			0.75	0.43	2.00

To remove excess inorganic carbon, filters were treated with HCl fumes for 24 h. A cocktail (8 mL, Ecolite) was added to the vials and radioactivity was determined in a liquid scintillation counter (Beckmann).

Depth-integrated values of PP (mg C m^{-2} h^{-1}) were estimated using trapezoidal integration over the euphotic zone (25–30 m), with the exception of Central Patagonia, where the sampling depth reached only the upper 10 m. Integrated production rates per hour were multiplied by daily light hours for the Chilean fjords and are given in mg C m^{-2} d^{-1} (spring–summer: 9 h; Iriarte et al., 2001, 2007). Integrated production rates given per hour in the literature were multiplied by daily light hours. For nutrients, nitrate, orthophosphate, and silicic acid concentrations (μM) were averaged for the upper 25 m of the water column in all four zones.

Although most information on PP and nutrients was available for the spring period (September through December) in all areas, we also included summer PP data published by Magazzù et al. (1996) for Southern Patagonia and unpublished summer PP data for the Inner Sea of Chiloé and Northern Patagonia.

3.2. Sediment data

The sedimentological characterization of the Chilean fjords was based on a total of 118 sediment stations. The major contribution to this information came from 74 stations sampled by the *CIMAR* cruises *7* and *10* (Inner Sea of Chiloé); *4*, *7*, and *8* (Northern Patagonia); *2* (Central Patagonia), and *3* (Magellan Strait). Additionally, new data were included for 26 sediment stations that were sampled by other cruises in the fjord region: *Beagle expedition* (2003), *Palmer NBP0505* (2005), *Gran Campo II* (2005 and 2007), *PACHIDERME* (2007), *Reloncaví* (2008), *Baker/Tortel* (2008), and *Mirai MR08-06* leg 2 (2009) (Table 2).

Table 3 presents the stations and locations within each of the four zones: 37 stations in the Inner Sea of Chiloé, 33 in Northern Patagonia, and 24 stations each in Central and Southern Patagonia. For the first two zones (Inner Sea of Chiloé, Northern Patagonia), published data were used for biogenic opal (Rebolledo, 2007; Silva et al., 2009), organic carbon (C_{org}), molar C/N (Sepúlveda, 2005; Rojas and Silva, 2005; Silva, 2008; Silva et al., 2009), and bulk sedimentary $\delta^{13}C_{org}$ (Pinto and Bonert, 2005; Sepúlveda, 2005; Silva et al., 2009; Rebolledo et al., this issue). Information for Central and Southern Patagonia relied on the publications of Baeza (2005) and Silva (2008), and largely on unpublished data (Table 2). For these zones, biogenic opal data were new and are reported as $\%Si_{OPAL}$.

Biogenic opal was determined following the methodology of Mortlock and Froelich (1989), which consists of the extraction of silica with an alkaline solution at 85 °C for 6 h, and measuring dissolved silicon concentrations in the extracts by spectrophotometry at 812 nm.

Most of the sediment information reported here refers to surface sediments collected with box-, multi-, Rhumor-, or Haps

Table 2
Sediment stations and data sources used for biogenic opal, organic carbon (C_{org}), molar C/N, and carbon stable isotope $\delta^{13}C$ in surface sediments from Patagonia. Data sources: 1: Silva et al. (2009), 2: Rebolledo et al. (this issue), 3: Rebolledo et al. (2005), 4: Rebolledo (2007), 5: Rebolledo et al. (2008), 6: Sepúlveda (2005), 7: Silva (2008), 8: Caniupán (pers. comm.); 9: Harada (pers. comm.); 10: Kilian (pers. comm.); 11: Bertrand (pers. comm.); 12: Baeza (2005), 13: Rojas and Silva (2005; *data taken from figures); 14: Pinto and Bonert (2005).

Zone	Location	Cruise	Station	Ref opal	Ref C/N and C_{org}	Ref $\delta^{13}C$
Inner Sea of Chiloé	Reloncaví Fjord	*CIMAR 10*	4	1	1	1
	Reloncaví Fjord	*CIMAR 10*	5	1	1	
	Reloncaví Fjord	*CIMAR 10*	6	1	1	1
	Reloncaví Fjord	*CIMAR 10*	7	1	1	1
	Reloncaví Fjord	*Reloncaví*	6B	This study	This study	1
	Reloncaví Sound	*CIMAR 10*	1	1	1	1
	Reloncaví Sound	*CIMAR*	10	2	1	1
	Reloncaví Sound	*CIMAR*	10	3	1	1
	Reloncaví Sound	*CIMAR 10*	8	1	1	1
	Reloncaví Sound	*PACHIDERME*	MD07-3102CQ	This study	This study	
	Ancud Gulf	*CIMAR 10*	10	1	1	1
	Ancud Gulf	*CIMAR 10*	12	1	1	1
	Ancud Gulf	*CIMAR 10*	13	1	1	
	Ancud Gulf	*CIMAR*	10	14	1	1
	Ancud Gulf	*CIMAR*	10	15	1	1
	Ancud Gulf	*CIMAR 10*	16	1	1	1
	Ancud Gulf	*CIMAR 10*	17	1	1	1
	Ancud Gulf	*CIMAR 10*	20	1	1	1
	Ancud Gulf	*CIMAR 10*	21	1	1	
	Ancud Gulf	*CIMAR 10*	22	1	1	1
	Ancud Gulf	*CIMAR 10*	24	1	1	1
	Ancud Gulf	*CIMAR 10*	25	1	1	
	Ancud Gulf	*CIMAR 10*	26	1	1	
	Ancud Gulf	*CIMAR 10*	27	1	1	1
	Ancud Gulf	*CIMAR 10*	28	1	1	
	Ancud Gulf	*CIMAR 10*	29	1	1	1
	Ancud Gulf	*CIMAR 10*	30	1	1	
	Ancud Gulf	*CIMAR 10*	41	1	1	
	Ancud Gulf	*PACHIDERME*	MD07-3109H	2	2	
	Comau Fjord	*CIMAR 10*	18	1	1	1
	Comau Fjord	*CIMAR 10*	19	1	1	1
	Corcovado Gulf	*CIMAR 10*	35	1	1	1
	Corcovado Gulf	*CIMAR 10*	37	1	1	1
	Corcovado Gulf	*CIMAR 10*	39	1	1	1
	Corcovado Gulf	*CIMAR 10*	43	1	1	1
	Corcovado Gulf	*CIMAR 10*	46	1	1	
	Guafo Mouth (oceanic)	*CIMAR 7*	1	1	1	1
Northern Patagonia	N entrance Moraleda Channel	*CIMAR 7*	6	1	1	1
	N entrance Moraleda Channel	*CIMAR 8**	6		13	
	N entrance Moraleda Channel	*CIMAR 4*	6			14
	Moraleda Channel	*CIMAR 8**	8		13	
	Moraleda Channel	*CIMAR 8**	9		13	
	Moraleda Channel	*CIMAR 8**	11		13	
	Moraleda Channel	*CIMAR 8**	14		13	
	Moraleda Channel	*CIMAR 4*	11			14
	Moraleda Channel	*CIMAR 4*	14			14
	Jacaf Fjord	*CIMAR 7*	BC 33	3	6	6
	Jacaf Fjord	*CIMAR 7*	PC 33	5	6	6
	Jacaf Fjord	*CIMAR 7*	36		6	6
	Puyuhuapi Fjord	*CIMAR 7*	BC 35	3	6	6
	Puyuhuapi Fjord	*CIMAR 7*	BC 40	3	6	6
	Puyuhuapi Fjord	*CIMAR 7*	42	6	6	
	Puyuhuapi Fjord	*CIMAR 7*	39	6	6	
	Aysén Fjord	*PACHIDERME*	MD07-3113H	This study	This study	
	Aysén Fjord	*CIMAR 8**	17A		13	
	Aysén Fjord	*CIMAR 4*	17A			14
	Aysén Fjord	*CIMAR 4*	19			14
	Aysén Fjord (head)	*CIMAR 4*	21			14
	Quitralco Fjord	*CIMAR 7*	PC 29A	4	4	
	Quitralco Fjord	*CIMAR 7*	BC 29 A	4	6	6
	Quitralco Fjord	*CIMAR 7*	29		6	6
	Quitralco Fjord	*CIMAR*	7 30A		6	6
	Quitralco Fjord	*CIMAR 7*	30		6	6
	Cupquelán Fjord	*CIMAR 7*	28		6	6
	Cupquelán Fjord	*CIMAR 7*	27	6	6	
	King Channel	*CIMAR 8**	51		13	
	King Channel (Oceanic)	*CIMAR 8**	53		13	
	Memory Channel	*CIMAR 8**	54		13	
	Chacabuco Channel	*CIMAR 8**	72		13	
	Pulluche Channel	*CIMAR 8**	76		13	
Central Patagonia	Tortel	*Baker/Tortel*	8	This study	This study	This study
	Steffen Fjord	*CIMAR 2*	11		7	
	Steffen Fjord	*CIMAR 2*	12		7	

Table 2 (*continued*)

Zone	Location	Cruise	Station	Ref opal	Ref C/N and C_{org}	Ref $\delta^{13}C$
	Steffen Fjord	*CIMAR 2*	13		7	
	Steffen Fjord	*CIMAR 2*	14		7	
	Mitchell Fjord (head)	*CIMAR 2*	16		7	
	Baker Channel (head)	*CIMAR 2*	10		7	
	Baker Channel	*Mirai*	MUC 40	This study	This study	This study
	Baker Channel	*CIMAR 2*	6		7	
	Baker Channel	*CIMAR 2*	7		7	
	Baker Channel	*CIMAR 2*	8		7	
	Baker Channel	*CIMAR 2*	9		7	
	Baker Channel (oceanic)	*CIMAR 2*	5		7	
	Penguin Sound	*CIMAR 2*	34		7	
	Europa Sound	*CIMAR 2*	36		7	
	Europa Sound	*CIMAR 2*	39		7	
	Icy Channel	*Palmer*	JPC 42	This study	7	
	Icy Channel	*Palmer*	KC 41	This study	7	
	Icy Channel	*CIMAR 2*	31		7	
	Icy Channel	*CIMAR 2*	35		7	
	Concepción Channel	*PACHIDERME*	MD07-3124	This study	8	
	Concepción Channel	*CIMAR 2*	40		7	
	Concepción Channel	*CIMAR 2*	42		7	
	Concepción Channel (oceanic)	*CIMAR 2*	43		7	
Southern Patagonia	W entrance Magellan Strait	*Beagle*	MUC 3	This study	9	9
	W entrance Magellan Strait	*Beagle*	PC 3	This study	9	9
	W entrance Magellan Strait	*CIMAR 3*	12		7	
	W entrance Magellan Strait	*CIMAR 3*	13		7	
	Paso del Mar	*Gran Campo II*	CHRR	This study	10	
	Paso del Mar	*Gran Campo II*	TA-1		12	
	Skyring Sound	*Gran Campo II*	SKY-E1		12	
	Williams Bay	*Gran Campo II*	BW		12	
	Escarpada	*Gran Campo II*	ES		12	
	Vogel	*Gran Campo II*	VO-1		12	
	Inutil Bay in Skyring Sound	*Gran Campo II*	IN-1		12	
	Gajardo Channel	*Gran Campo II*	CG-1		12	
	Zañartu Island (central)	*Gran Campo II*	ZA-CE		12	
	Zañartu Island (south)	*Gran Campo II*	ZA-SU		12	
	Andrés Inlet	*Gran Campo II*	AN-1		12	
	Carlos III Island	*CIMAR 3*	10		7	
	Central Magellan Strait	*CIMAR 3*	54		7	
	Central Magellan Strait	*CIMAR 3*	55		7	
	Central Magellan Strait	*PACHIDERME*	MD07-3132	This study	10	
	Central Magellan Strait	*Beagle*	MUC 4	This study	7	
	Central Magellan Strait	*Beagle*	PC 4	This study	7	
	Inutil Bay	*CIMAR 3*	56		7	
	Inutil Bay	*CIMAR 3*	57		7	
	Marinelli Fjord	*Palmer*	JPC 67	This study	11	11

corers. In a few cases, it also includes the uppermost cm of sediments collected with gravity and/or piston corers (e.g., MD07-3102CQ, MD07-3124, MD07-3132, JPC 42, JPC 67; Table 2).

In order to represent the spatial distribution of selected variables (i.e. silicic acid, $\%Si_{OPAL}$, $\%C_{org}$, and bulk sedimentary $\delta^{13}C_{org}$) the software Ocean Data View 4 was used with a coastline extracted from the optional package odvOP_coast_SouthAmerica_w32.exe. The graphic representation of the data was constructed with a VG gridding. This exercise was restricted to the Inner Sea of Chiloé and Northern Patagonia zones since these two zones have the best sampling coverage.

4. Results

4.1. Water column

Water column primary production (PP) and nutrient concentrations are described for the four zones for the spring period (Table 1; Fig. 3). Water column data for each station were averaged by location: 7 locations in the Inner Sea of Chiloé, 11 in Northern Patagonia, 10 in Central Patagonia, and 7 in Southern Patagonia (Table 1).

Following the transect from 41° to 55°S (Table 1; Fig. 3), very high PP values were measured at locations within the Inner Sea of Chiloé (range in spring = ~1100–4800 mg C m^{-2} d^{-1}; range in summer = ~2300–9000 mg C m^{-2} d^{-1}) with the exception of the Guafo Mouth, where the lowest spring production was observed (134 mg C m^{-2} d^{-1}). In Northern Patagonia, maxima (>2200 mg C m^{-2} d^{-1}) corresponded to Moraleda Channel (spring and summer), Aysén Fjord (summer), and Quitralco Fjord (spring), and the lowest spring values were observed in Jacaf fjord and in the confluence between the Jacaf and Puyuhuapi fjords (<300 mg C m^{-2} d^{-1}). In Central Patagonia, the lowest spring PP (91 mg C m^{-2} d^{-1}) was recorded in Caleta Tortel. Moderately low values characterized Steffen Fjord and Messier Channel (345 and 463 mg C m^{-2} d^{-1}, respectively), whereas all other locations within this zone were more productive (≥800 mg C m^{-2} d^{-1}). No data were available for the summer period in Central Patagonia. Within the Magellan Strait region in Southern Patagonia, PP values were high in spring (~1700 mg C m^{-2} d^{-1}), with the exception of Paso del Mar, where estimates were one order of magnitude lower. Summer values ranged between 344 and 681 mg C m^{-2} d^{-1}.

With respect to the north–south spatial distribution of nutrient concentrations in spring (Table 1; Fig. 3), nitrate and orthophosphate were highest in the Inner Sea of Chiloé

Table 3
Sediments. Averaged values of biogenic opal (%Si_{OPAL}), organic carbon (C_{org}%), molar C/N, and carbon stable isotope δ^{13}C for surface sediments of each location within each of the four zones: Inner Sea of Chiloé; Northern, Central, and Southern Patagonia. Blank spaces = no data.

Zone	Location	No. of stations	%Si_{OPAL}	C_{org} (%)	C/N (molar)	$\delta\,^{13}$C (‰)
Inner Sea of Chiloé	Reloncaví Fjord	5	6.47	1.26	10.73	−23.99
	Reloncaví Sound	5	10.26	1.62	8.59	−20.81
	Comau Fjord	2	5.56	1.89	12.10	−23.92
	Ancud Gulf	19	6.29	1.18	8.71	−20.95
	Corcovado Gulf	5	3.34	0.50	8.44	−21.09
	Guafo Mouth (Oceanic)	1		1.00	9.59	−19.11
Northern Patagonia	N entrance Moraleda Channel	3		1.57	8.42	−18.53
	Moraleda Channel	6		1.54	7.70	−16.81
	Jacaf Fjord	3	8.79	2.97	12.08	−22.76
	Puyuhuapi Fjord	4	4.47	2.53	13.89	−24.60
	Aysén Fjord	5	11.78	1.72	8.22	−22.90
	Quitralco Fjord	5	12.75	1.62	12.07	−23.04
	Cupquelán Fjord	2		0.67	15.06	−25.13
	Oceanic Sites	5		1.00	7.06	
Central Patagonia	Tortel	1	1.25	0.79	22.93	−26.09
	Steffen Fjord	4		0.25	11.10	
	Mitchell Fjord (head)	1		0.40	6.67	
	Baker Channel (head)	1		0.34	7.93	
	Baker Channel	5	3.51	0.77	10.80	−20.34
	Baker Channel (oceanic)	1		1.07	7.80	
	Penguin Sound	1		0.45	6.56	
	Europa Sound	2		0.38	6.77	
	Icy Channel	4	4.24	1.10	8.00	
	Concepción Channel	3	3.55	2.14	6.96	
	Concepción Channel (oceanic)	1		0.92	6.31	
Southern Patagonia	W entrance Magellan Strait	4	1.38	1.23	8.21	−19.77
	Paso del Mar	2	4.68	10.32	13.47	
	Skyring Sound Area	9		3.40		
	Carlos III Island	1		1.10	8.02	
	Central Magellan Strait	5	4.90	1.21	8.00	
	Inutil Bay	2		0.98	7.70	
	Marinelli Fjord	1	3.14	1.03	10.89	−22.17

(Reloncaví Sound: 8.38 μM for NO_3^- and 1.14 μM for PO_4^{-3}; Corcovado Gulf: 12.04 and 1.57 μM) and in Northern Patagonia (Costa Channel: 11.50 and 1.30 μM; Quitralco Fjord: 11.40 and 1.23 μM; Elefantes Gulf: 10.67 and 1.17 μM). In Central Patagonia, Eyre Sound had the highest nitrate concentration (7.28 μM), and orthophosphate was maximal in Penguin Sound (1.52 μM). In Southern Patagonia, these nutrients were higher in the western and central section of the Magellan Strait ($>$5 μM for NO_3^- and $>$0.7 μM for PO_4^{-3}), whereas the lowest values corresponded to Marinelli Fjord in the eastern section of the strait. High silicic acid concentrations characterized the locations at the fjord heads and close to important river discharges in the Inner Sea of Chiloé and Northern and Central Patagonia: Reloncaví (23.81 μM) and Aysén fjords (34.03 μM), and Tortel (19.50 μM). Compared to the previous three zones, values were much lower (~2–7 μM) in Southern Patagonia.

4.2. Sediments

The four zones were also described in terms of C_{org} and Si_{OPAL} contents, molar C/N, and the carbon stable isotope δ^{13}C of surface sediments (Table 3; Fig. 4). Sediment data for each station were averaged by location, with 6 locations for the Inner Sea of Chiloé, eight for Northern Patagonia, 11 for Central Patagonia, and seven for Southern Patagonia (Table 3). All locations were organized from N to S in the same fashion as was done for the water column (transect from 41° to 55°S).

C_{org} and Si_{OPAL} served as proxies of export production from the water column to the sediments, whereas molar C/N and the stable carbon isotope signature δ^{13}C were used as proxies of the origins of sedimentary organic matter (Sepúlveda et al., this issue). Stable isotope (δ^{13}C) information was very scarce and mainly restricted to the sediments of the Inner Sea of Chiloé and Northern Patagonia; only two values were available for each Central and Southern Patagonia (Table 3).

The Si_{OPAL} content was generally $>$5% in the Inner Sea of Chiloé and Northern Patagonia and $>$10% in Reloncaví Sound and the fjords Aysén and Quitralco. In Central and Southern Patagonia, Si_{OPAL} contents decreased abruptly (range 1–5%), with maxima in the Icy Channel and in the Central Magellan Strait (Table 3; Fig. 4).

The Chilean fjords were rich in C_{org} and high values ($\geq$1%) were observed in all zones except Central Patagonia, where such values were limited to locations far away from glacier influence (e.g., Concepción Channel). In each of the other three zones, locations within a fjord (e.g., Comau, Jacaf, Puyuhuapi, $>$1–3%) and/or in the semi-enclosed and protected basins of Paso del Mar and Skyring Sound ($>$3–10%) had the highest C_{org} contents (Table 3; Fig. 4).

Molar C/N showed the highest values (~10–23; Table 3) at locations adjacent to the continent with an important river influence and/or in the vicinity of glaciers, especially in the Reloncaví (10.73), Comau (12.10), Jacaf (12.08), Puyuhuapi (13.89), Quitralco (12.07), and Cupquelán (15.06) fjords of the Inner Sea of Chiloé and Northern Patagonia; in Caleta Tortel (22.93) and Steffen Fjord of Central Patagonia (11.10); and in Marinelli Fjord (10.89) and the protected area of Puerto Churruca (13.47) in Southern Patagonia. Bulk sediment $\delta^{13}C_{org}$ ranged between −16.81 (Moraleda Channel) and −26.09 (Caleta Tortel) (Table 3; Fig. 4); in general, more negative values were observed at the fjord heads.

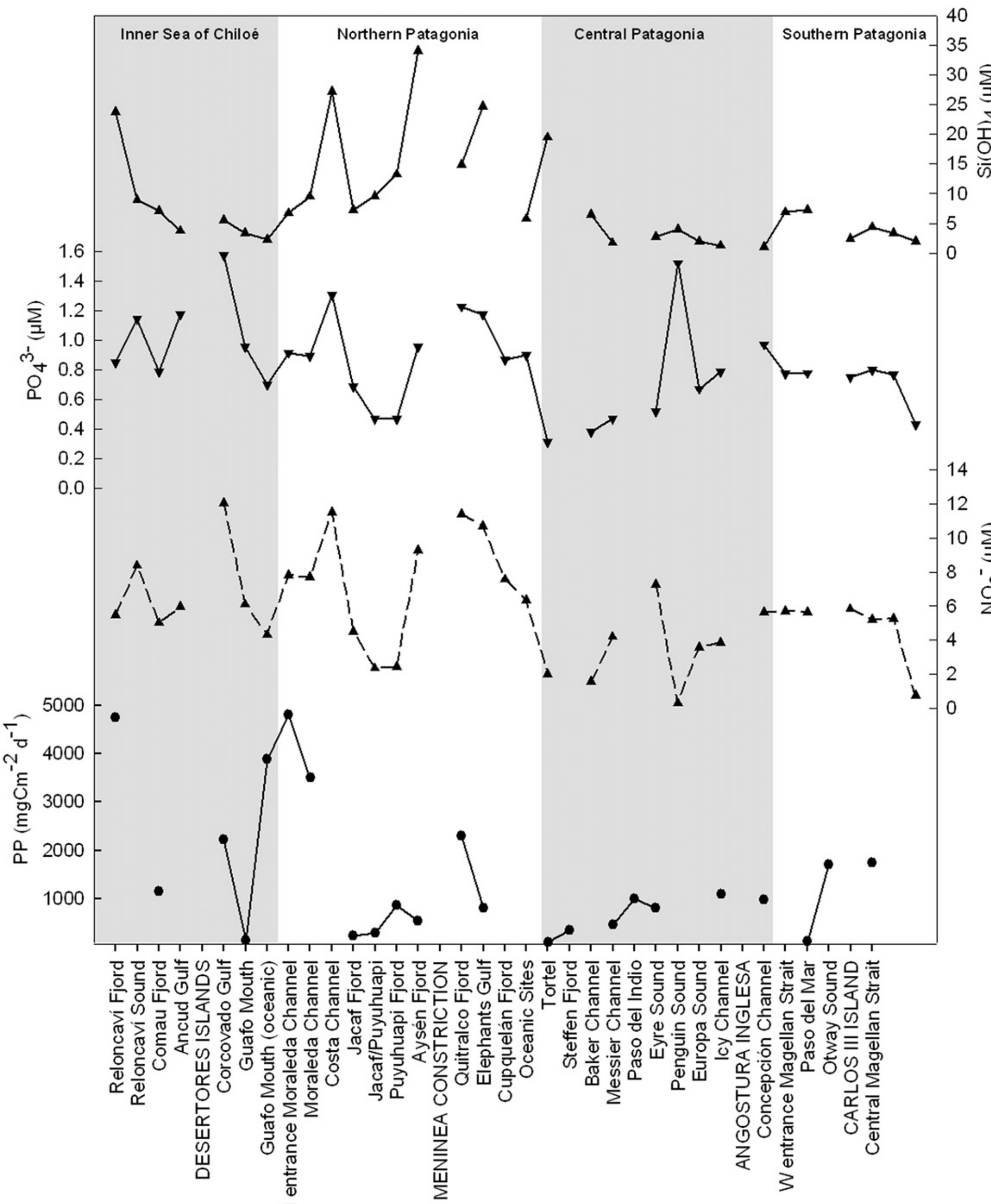

Fig. 3. Water column. Primary production and nutrient concentrations in spring for the four zones. The locations are organized from N to S, from 41°S (Reloncaví Fjord) to 55°S (Marinelli Fjord). The values are averages of all the stations within each location (see Table 1).

5. Discussion

The Chilean Patagonia coastal area is a vast region that represents a junction between the coastal ocean and the freshwater systems on the continent. The river regimen varies with latitude, and three kinds of regimens can be found, i.e., winter-centered pluvial (to the north of 43°S), summer-centered nival (south of 47°S), and mixed pluvial–nival (43–47°S) (Fernández and Troncoso, 1984; Dávila et al., 2002).

The area has a typical estuarine circulation pattern determined by an offshore surface flow of freshwater over an onshore flow of oceanic water. The surface freshwater layer is separated from the marine layer by a strong pycnocline, resulting in overlapping brackish and marine characteristics in the fjord ecosystem. The productivity of the Chilean fjords is influenced by the combined effect of important contributions of dissolved silicon from freshwater discharge (river runoff, glacial melting) as well as the vertical entrainment of sub-Aantarctic Water, which carries macronutrients (nitrate, orthophosphate) from the adjacent oceanic area (Silva et al., 1997, 1998; Iriarte et al., 2007; Vargas et al., this issue). In spring–summer, a north–south decreasing trend in the average particulate organic carbon concentrations of the upper 50 m of the water column has been observed from the Reloncaví area (200–600 mg C m^3; González et al., 2010) to the Magellan Strait (76 C m^3; Fabiano et al., 1999). In general, the organic carbon

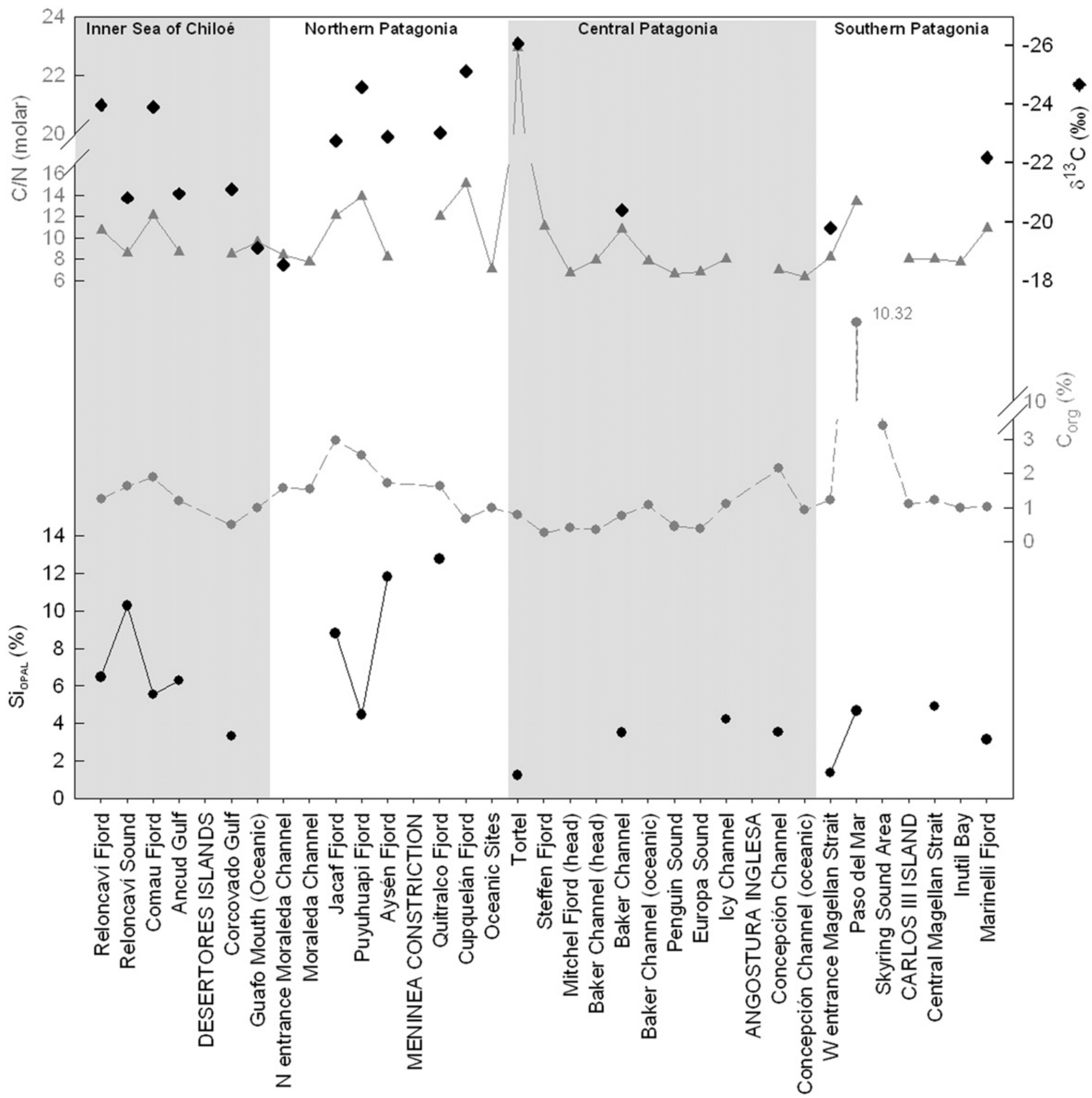

Fig. 4. Sediments. Percent biogenic opal (Si_{OPAL}) and organic carbon (C_{org}), molar C/N, and bulk sedimentary $\delta^{13}C$ (black diamonds) for the four zones. The locations are organized from N to S, from 41°S (Reloncaví Fjord) to 55°S (Marinelli Fjord). The values are averages of all stations within each location (see Tables 2 and 3).

content in the surface sediments reflects this southerly decrease (Silva and Prego, 2002).

We summarize all water column and sediment data with the aim of characterizing each of the four zones (Inner Sea of Chiloé; Northern, Central, and Southern Patagonia) in terms of productivity and its imprint in the surface sediments. For this purpose, all locations are averaged by zone (Table 4; Fig. 5).

5.1. Water column

The Inner Sea of Chiloé and Northern Patagonia are the zones with the highest PP spring and summer values (2428–5860 and 1667–2617 mg C m^{-2} d^{-1}, respectively), and also with the highest nutrient concentrations (Table 4). In the literature, these two zones are considered to be very productive marine systems in terms of phytoplankton and zooplankton biomass (e.g., Iriarte et al., 2007; Palma, 2008). Here, the latitudinal changes observed in PP seem to be tied to seasonal patterns in the light regime (González et al., 2010). In the Inner Sea of Chiloé, for example, González et al. (2010) show that the higher solar radiation and extended photoperiod of spring promote the growth of chain-forming diatoms in the water column. During spring in the Inner Sea of Chiloé, Iriarte et al. (2007) and González et al. (2010) note that micro-phytoplankton (mainly the chain-forming diatoms *Skeletonema*, *Chaetoceros*, and *Thalassiosira*) account for a significant portion of the biomass (> 60%), whereas nanoplankton dominate during post-bloom events and winter months. In Aysén fjord in Northern Patagonia, the micro-phytoplankton fraction contributes 77% and 40% to the mean total chlorophyll concentrations in spring (6.9 ± 3.3 mg m^{-3}) and summer (3.1 ± 1.2 mg m^{-3}) and the dominant diatom species are *Skeletonema costatum* and *Guinardia delicatula* (Pizarro et al., 2005).

Central Patagonia, on the other hand, shows the lowest average PP value for the entire Patagonia (spring PP= ~680 mg C m^{-2} d^{-1}; Table 4), although this may be an underestimation since information is only available for spring and the integration depth reaches only the upper 10 m of the water column (see Section 3). In general, mean chlorophyll concentrations in spring for the area between 47° and 52°S are lower (1.3 ± 3.3 mg m^{-3}) than further north, although highly variable (Pizarro et al., 2005). Given sufficient light for photosynthesis in spring–summer,

Table 4
Summary of water column and sediment data in the four zones (mean, standard deviation, minimum,and maximum values). Primary production, nitrate, orthophosphate, and silicic acid represent spring values. Summer primary production data are not available for Central Patagonia.

Zone		PP ($mg\,C\,m^{-2}\,d^{-1}$)		Nutrients in spring			$\%Si_{OPAL}$	C_{org} (%)	C/N (molar)	$\delta^{13}C$ (‰)
		Spring	Summer	NO_3^- (μM)	PO_4^{-3} (μM)	$Si(OH)_4$ (μM)				
Inner Sea of Chiloé	Mean	2427.98	5860.17	6.76	1.03	7.85	6.39	1.24	9.69	−21.64
	Std. dev.	1900.46	5015.75	2.65	0.30	7.41	2.50	0.48	1.46	1.93
	Min.	134.10	2313.50	4.32	0.70	2.25	3.34	0.50	8.44	−023.99
	Max.	4754.41	9406.84	12.04	1.57	23.81	10.26	1.89	12.10	−19.11
Northern Patagonia	Mean	1667.66	2616.86	7.42	0.89	15.32	9.45	1.70	10.56	−21.97
	Std. dev.	1702.03	1284.77	3.27	0.28	9.89	3.72	0.75	3.08	3.11
	Min.	235.80	1424.00	2.36	0.47	5.81	4.47	0.67	7.06	−25.13
	Max.	4812.64	4381.00	11.50	1.30	34.03	12.75	2.97	15.06	−16.81
Central Patagonia	Mean	680.58		3.56	0.70	4.84	3.14	0.78	9.26	−23.21
	Std. dev.	382.66		2.26	0.40	6.19	1.30	0.54	4.82	4.07
	Min.	91.00		0.30	0.31	1.00	1.25	0.25	6.31	−26.09
	Max.	1093.50		7.28	1.52	19.50	4.24	2.14	22.93	−20.34
Southern Patagonia	Mean	1183.89	418.04	4.73	0.72	4.39	3.52	2.75	9.38	−20.97
	Std. dev.	933.67	188.94	1.97	0.14	2.23	1.63	3.44	2.32	1.70
	Min.	106.00	238.64	0.75	0.43	2.00	1.38	0.98	7.70	−22.17
	Max.	1741.67	681.48	5.83	0.80	7.25	4.90	10.32	13.47	−19.77

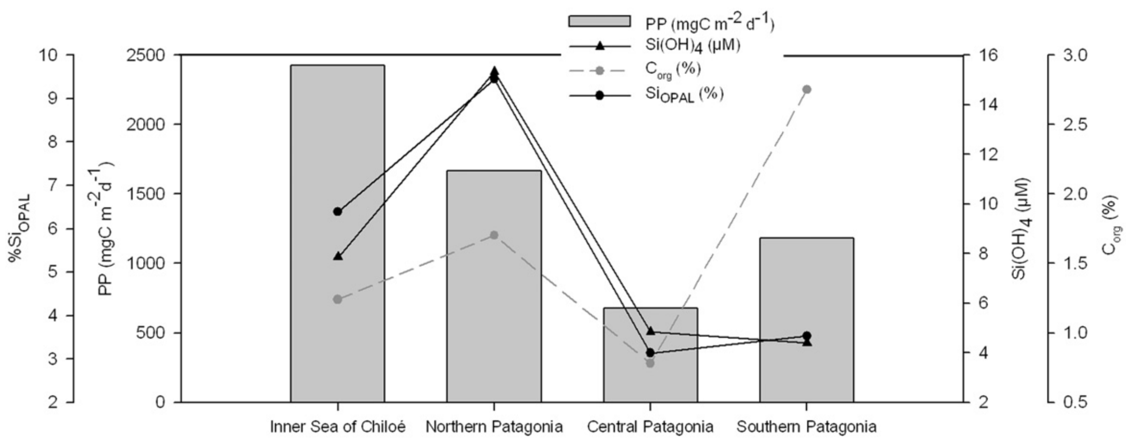

Fig. 5. Comparison between spring primary production (PP) and silicic acid ($Si(OH)_4$) in the water column, and biogenic opal ($\%Si_{OPAL}$) and organic carbon ($\%C_{org}$) from surface sediments in the four zones: Inner Sea of Chiloé, Northern, Central, and Southern Patagonia. All locations were averaged by zone (see Table 4).

diatom concentrations may reach 1.8×10^6 cells L^{-1}, as they did in spring in Golfo Almirante Montt (51°46′S 72°57′W) (Alves-de-Souza et al., 2008). This value falls within the ranges of spring values from the Inner Sea of Chiloé ($3–10\times10^6$ cells L^{-1} in Reloncaví Fjord) and between Desertores Islands and the Guafo Mouth ($0.1–1\times10^6$ cells L^{-1}; González et al., 2010).

Central Patagonia is an interesting area that differs from the Inner Sea of Chiloé and the Northern Patagonia zones in terms of its extensive ice coverage and major rivers. On the mountain side, this zone includes the Northern and Southern Patagonian Icefields, with several glaciers that descend towards the coastline, breaking up at the fjord heads and creating icebergs that dilute the salty waters upon melting (Silva and Calvete, 2002). These icebergs release inorganic matter known as glacial silt (giving the appearance of milky fjord waters) that attenuates PP due to decreased light penetration (Montecino and Pizarro, 2008). In fact, the lowest spring PP value is observed in Caleta Tortel (91 $mg\,C\,m^{-2}\,d^{-1}$; Table 4). The area also includes the Baker River (1133 $m^3\,s^{-1}$), which empties into Baker Channel near the village of Caleta Tortel and the Pascua River (753 $m^3\,s^{-1}$), which flows into Mitchell Fjord. The Baker River is Chile's largest river in terms of water volume, and its characteristic turquoise-blue color is due to the glacial sediments deposited therein.

Data for the Southern Patagonia zone includes the western (from the Pacific Ocean opening to Carlos III Island) and central (from Carlos III Island to Segunda Angostura) microbasins of the Magellan Strait and an adjacent sound (Otway), bay (Inútil), and fjord (Marinelli) (Fig. 2). The constriction-sill (about 100 m deep) located off Isla Carlos III acts as a physical barrier that impedes the entry of Modified sub-Antarctic Water and sub-Antarctic Water from the Pacific into the central microbasin (Valdenegro and Silva, 2003). The Magellan Strait region is affected by strong winds from the northwest or west and is characterized by a marked W–E gradient in precipitation and by light limitation (normally cloud-covered for 6–8 months) (Iriarte et al., 2001, and references therein; Schneider et al., 2003).

Average PP values for spring and summer are ~1184 and 418 $mg\,C\,m^{-2}\,d^{-1}$, respectively. The lowest PP is observed in spring in Paso del Mar (106 $mg\,C\,m^{-2}\,d^{-1}$) and the highest off Punta Arenas (3322 $mg\,C\,m^{-2}\,d^{-1}$) (Table 4). The highest concentrations of phytoplankton are recorded in spring–summer (~1×10^6 cells L^{-1}; Alves-de-Souza et al., 2008). Iriarte et al. (1993) and Magazzù et al. (1996) report dominant micro-phytoplankton in spring and pico- and nanoplankton in summer–autumn. In this area, the important diatom genera include *Chaetoceros*, *Thalassiosira*, *Rhizosolenia*, *Leptocylindrus*, *Pseudo-nitzschia*, and *Thalassionema*. Both biomass and primary production distributions are influenced by exchange mechanisms with the ocean at the western opening of the Magellan Strait and along the Pacific arm, tidal dynamics, glacio-fluvial contributions, and the presence of a thermohaline front near Carlos III Island (Magazzù et al., 1996; Torres et al., this issue). This physical scenario might have direct effects on the structure and functioning of the phytoplankton assemblages (Torres et al., this issue) and the export of PP out of the euphotic zone.

Nitrate and orthophosphate concentrations in the Magellan area are rather uniform ($\sim$5 and $\sim$0.7 μM, respectively), with the exception of Marinelli Fjord, where the lowest concentrations are measured (Table 1). In contrast, silicic acid shows a W–E gradient, with relatively higher concentrations in the western section ($\sim$7 μM) than in the central Magellan microbasin (2.5–4.4 μM), and the lowest value in Marinelli Fjord (Table 1).

The data on inorganic nutrients in the four zones reveal waters with a low NO_3^-:PO_4^{-3} ratio (<9), as previously reported by Iriarte et al. (2007) for the Inner Sea of Chiloé; these authors suggest that the phytoplankton assemblages (diatoms) would first deplete NO_3^- (as opposed to orthophosphate) from the water column. Therefore, nitrogen physiology may be important to the dynamics of phytoplankton blooms in spring and summer in the Patagonian fjords. Iriarte et al. (2007) propose that the low concentration of inorganic nitrogen through the water column may be explained by phytoplankton uptake and/or by the mixing of freshwater with low nutrient contents, as documented along the shelf margin of southern Chile (Silva et al., 1997). On the other hand, the lower silicic acid concentration in the Magellan area results in a decreased Si:N ratio (≤ 1) in spring and summer, suggesting that diatoms could deplete silicic acid from the water column before nitrate, thereby acting as a limiting nutrient for diatom growth in these coastal waters of Southern Patagonia, probably leading to less silicified diatom cells (Iriarte et al., 2001) or to proliferations of other phytoplankton groups such as dinoflagellates (Torres et al., this issue).

5.2. *The sedimentary signal*

Surface sediment C_{org} content for the entire study area range between 0.25% (Steffen Fjord) and 10.32% (Paso del Mar) (Table 3). Previous studies in the Patagonian fjords system conclude that the surface sediments are mostly marine in origin, with contributions from terrestrial materials that increase towards the heads of the fjords (e.g., Silva et al., 2001; Rojas and Silva, 2005). A recent study by Sepúlveda et al. (this issue) in Northern Patagonia shows that the contribution of marine-derived organic carbon varies widely, from 13% in Puyuhuapi Fjord at the Cisnes River outlet, to 75–90% at the mouths of the Jacaf, Puyuhuapi, and Quitralco fjords, to a maximum of 96% of the organic pool (at the northern entrance of Moraleda Channel). It is very common to find zones with high concentrations of organic matter in the sediments associated with high water column primary productivity (Silva and Prego, 2002).

Our results indicate that the overall PP pattern follows the patterns of organic carbon and biogenic opal contents in the sediments, i.e., the two zones with highest PP (Inner Sea of Chiloé and Northern Patagonia) are associated with high concentrations of C_{org} and Si_{OPAL} (Fig. 5). This overall picture agrees with the findings of Silva and Prego (2002). The exception is Southern Patagonia, where the average C_{org} is higher than in any other zone (2.75%; Table 4) due to the high organic carbon contents in Paso del Mar (Table 3), specifically at two sheltered sites: Tamar Island and Puerto Churruca. Si_{OPAL} contents in the surface sediments are almost twice as high in the Inner Sea of Chiloé and Northern Patagonia (6.39% and 9.45%, respectively) as in the other two zones (Table 4), and follow the latitudinal trend of C_{org} (except for Southern Patagonia) and the nutrients in the water column. Specifically, the silicic acid concentration agrees with the Si_{OPAL} in the sediments, showing the highest values in Northern Patagonia (Fig. 5), probably due to the close relation of diatoms with water column productivity and, hence, the preservation of Si_{OPAL} in the sediments. The water column silicic acid–sediment $\%Si_{OPAL}$ relation is also graphically represented in the maps of Fig. 6 (upper panel) for the Inner Sea of Chiloé and Northern Patagonia zones.

Organic carbon is lowest ($<0.5\%$) in the sediments of the Central Patagonian channels and fjords influenced by glaciers (Table 3) that deliver both cold freshwater (enhancing vertical stratification) and large amounts of clay and silt (diluting the organic content of the sediments) (Silva et al., 2001). On the other hand, C_{org} values $\geq 1\%$ characterize the sites beyond the glacial influence and adjacent to the ocean (e.g., Baker, Icy, and Concepción channels). The environmental conditions in this western area are less extreme than those previously mentioned: the western sites are free of cold freshwater and silt, light penetration is greater, and important nutrient input from the ocean favors primary production (Silva and Neshyba, 1979; Pizarro et al., 2000; Silva et al., 2001).

Circulation and water mass exchange between fjords and channels is limited by the presence of shallow sills (i.e., Desertores, Meninea, Angostura Inglesa, and Carlos III constrictions; Sievers and Silva, 2008), which may impose important contrasts among the four zones in terms of nutrient availability, primary production, and its export to the seafloor. Our compilation of data, however large, is too spotty and composed of many measurements taken in different years. Thus, it does not allow us to discuss the impacts that these topographic features may exert on both water column productivity and the imprint of this in the surface sediments. According to previous works, the signal of organic matter in the sediments seems to be more associated with the sediment texture than with the physical settings (e.g., Pinto and Bonert, 2005; Silva, 2008) – coarse sediments with low levels of total organic matter *vs.* fine sediments with high levels of total organic matter – except for clay–mud sediments in the vicinity of glaciers, where the contribution of inorganic matter from the erosion of rocks is highly significant (Silva, 2008 and references therein).

The elemental (C/N ratio) and stable isotope composition of organic carbon ($\delta^{13}C$) in the surface sediments can be used to trace the provenance of organic matter (e.g., Meyers, 1994, 1997). Although these two parameters are highly variable in the Inner Sea of Chiloé and the Northern Patagonian zones (Table 4), a simple linear regression shows a significant, positive association between molar C/N and $\delta^{13}C_{org}$ ($r^2=0.76$, $p=0$). These two zones include stations located at the fjord heads (e.g., Comau, Puyuhuapi) with important rivers that discharge allochthonous organic and inorganic material, translating into high C/N ratios and a more negative isotopic signal in the surface sediments (Table 3). This is clearly visualized in Fig. 6 (lower panel). Our results agree with previous studies that have shown that the carbon isotopic signal becomes lower towards the fjord heads (Pinto and Bonert, 2005), proving that the main input of organic matter at those sites originates in the fluvial discharge, whereas at sites with an oceanic influence, the prevailing source is marine (Table 3; Silva, 2008; Sepúlveda et al., this issue; Silva et al., this issue). In Central Patagonia, the highest molar C/N and most negative $\delta^{13}C_{org}$ values are found in Caleta Tortel (22.93‰ and -26.09‰, respectively; Table 3), a site directly influenced by the Steffen and Baker rivers and the Steffen Glacier. Relatively high C/N values (10.89) also

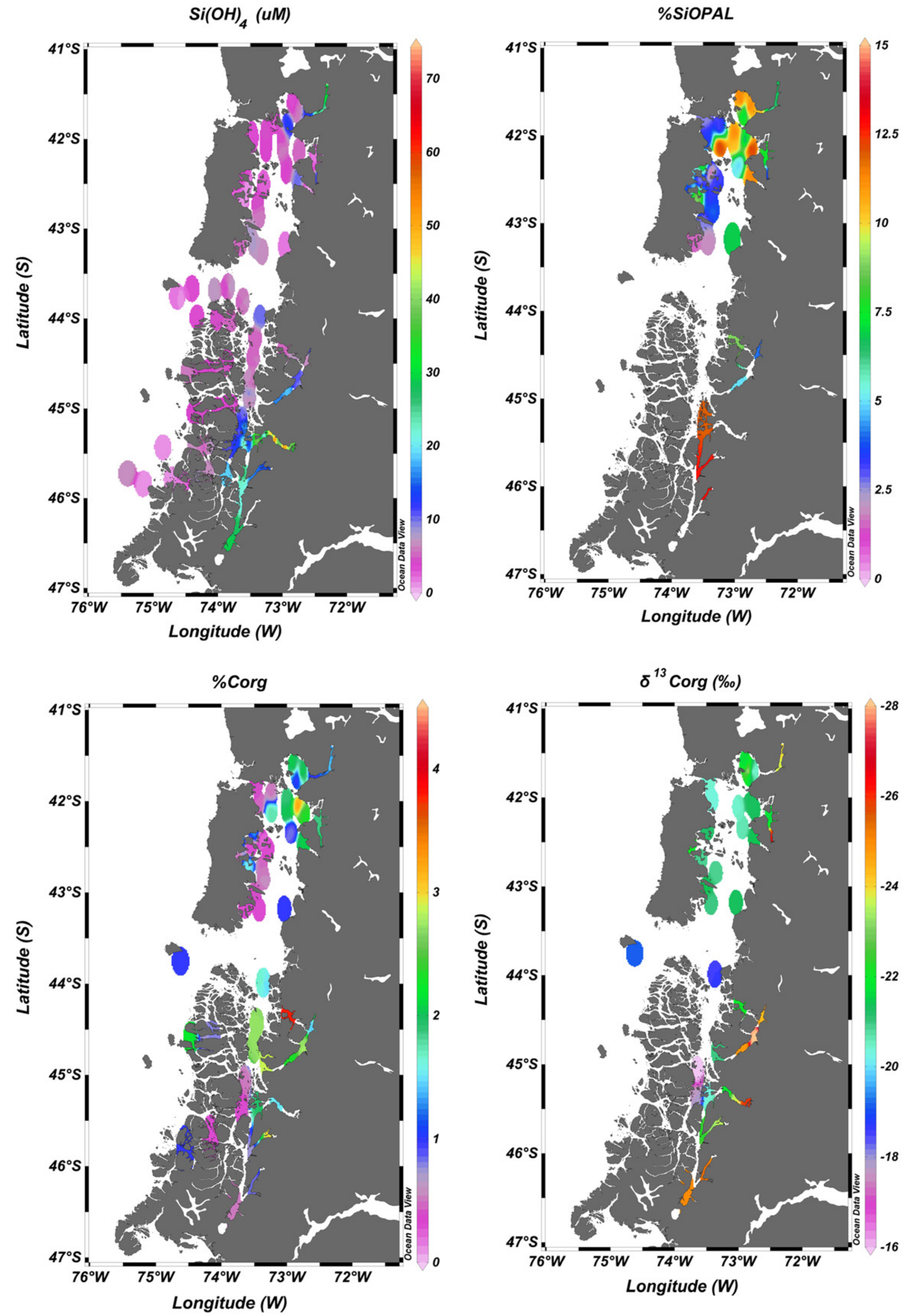

Fig. 6. Graphic representation (ODV 4) of the spatial distribution of silicic acid ($Si(OH)_4$, μM) in the water column, and sediment proxies percent biogenic silica (%Si_{OPAL}), percent organic carbon (%C_{org}), and bulk sedimentary $\delta^{13}C_{org}$ (‰) in the Inner Sea of Chiloé and Northern Patagonia zones.

characterize the Marinelli Fjord location in Southern Patagonia, where the Marinelli and Ainsworth glaciers are found, and the highest C/N corresponds to the Puerto Churruca site in Paso del Mar (13.47). The only two carbon isotopic values available for the Magellan Strait area show a strong influence of marine organic matter (-19.77‰ to -22.17‰; Table 3).

Table 5
Comparison of spring primary production (PP) and geochemistry of surface sediments from the Chilean fjord region (41–55°S, oceanic sites excluded) with other selected fjord systems. Primary production comparisons are limited to those areas where PP was measured in spring and given as integrated daily values over the euphotic zone since measurements from other fjord systems are very difficult to convert due to variable light and ice coverage.

Location	Reference	PP ($mg\,C\,m^{-2}\,d^{-1}$)	$\%Si_{OPAL}$	$\%C_{org}$	C/N	$\delta^{13}C$ (‰)
Balsfjord (Norway)	Archer et al. (2000)	1902–3820				
Malangen Fjord (Norway)	Archer et al. (2000)	1350–2480				
Ullsfjord (Norway)	Archer et al. (2000)	2060–4310				
Korsfjorden (Norway)	Erga and Heimdal (1984)	1200–1400				
Boknafjorden (Norway)	Erga (1989)	100–900[a]				
Gullmar Fjord (Sweden)	Lindahl et al. (1998)	600–1200				
Saanich Inlet (Canada)	Grundle et al. (2009)	1650–2440				
Inner fjords and off Spitsbergen (Norway)	Winkelmann and Knies, 2005			0.5–2.7	6.3–14.8	−21.1 to −25.2
Nordåsvannet Fjord (Norway)	Müller (2001)		~2[b,c]	12.4	12.7	−23.9
Framvaren Fjord (Norway)	Velinsky and Fogel (1999)			11.9	9.3	−25.1
Koljö Fjord (Sweden)	McQuoid and Nordberg (2003)			6		
Havsters Fjord (Sweden)	Gustafsson and Nordberg (2000)			2–4.1	9.6–11.4	
Kiel Fjord (SW Baltic Sea)	Nikulina et al. (2008)		0.1–8	1–7.8	4–15	
Flensburg Fjord (Germany and Denmark)	Nikulina and Dullo (2009)		2.3–5.2	7.1	10.5	
Upper Muir Inlet (SE Alaska)	Walinsky et al. (2009)		1.9[b]	0.3	11.5	−20.4
Lower Muir Inlet (SE Alaska)	Walinsky et al. (2009)		1.2[b]	0.3	9.9	−21.4
Upper Lynn Canal (SE Alaska)	Walinsky et al. (2009)		6.1[b]	0.8	10	−21.2
Lynn Canal (SE Alaska)	Walinsky et al. (2009)		15[b]	2.4	9.6	−20.4
Effingham Inlet (Canada)	Hay et al. (2009)		~18[c]	7.6	12.2	−23.3[c]
Saanich Inlet (Canada)	Calvert et al. (2001)		45[c]	3	9	
Saguenay Fjord (Canada)	St-Onge and Hillaire-Marcel (2001)			1.2–2.0[c]	15–25[c]	−20.4 to −26.5[c]
Chilean fjords						
Inner Sea of Chiloé	This study	1147–4754 (5476[d])	3.3–10.3	0.5–1.9	8.4–12.1	−20.8 to −23.9
Northern Patagonia	This study	235–4812	4.5–12.8	(0.5[e]) 0.7–2.9 (3.4[e])	7.7–15.0 (20.5[e])	−16.8 to −25.1 (−28.2[e])
Central Patagonia	This study	91–1094	1.3–4.2	0.2–2.1	6.3–22.9	−20.3 to −26.1
Southern Patagonia	This study	106–1742	1.4–4.9	0.9–10.3	7.7–13.4	−19.7 to −22.1

[a] Taken from graph (April through June).
[b] Reported as $OPAL = 2.4 \times \%Si_{OPAL}$.
[c] Surface sediment data taken from graphs.
[d] From González et al. (accepted).
[e] From Sepúlveda et al. (this issue).

5.3. Comparison with other fjord systems

Given the importance of high-latitude fjords as sites for carbon burial and CO_2 sequestration (e.g. Silva and Prego, 2002; Winkelmann and Knies, 2005; Sepúlveda et al., this issue; Torres et al., submitted), we compare our results from the Chilean fjord region with those of other fjord systems in the world (Table 5). Although published water column production data are scarce, high variability in primary production is evident for all fjord systems. The range of the Norwegian fjords (100–4310 $mg\,C\,m^{-2}\,d^{-1}$) falls within that of the spring values for the Chilean fjords (91–4812 $mg\,C\,m^{-2}\,d^{-1}$). High variability is also seen in the C_{org} contents of the surface sediments of most fjords, and the overall range in the Chilean fjords (0.2–10.3%) is most similar to that of the Norwegian fjords (0.5–12.4%). On the other hand, it is interesting to note that the C_{org} range in Central Patagonia resembles that of the Alaskan inlets, both fjord areas being strongly influenced by glaciated terrain (Table 5).

Biogenic silica produced by organisms with a siliceous skeleton (e.g., diatoms, silicoflagellates, radiolarian, sponges) is an important constituent of the Chilean fjord sediments (Si_{OPAL} overall average for all locations: 5.7 ± 3.4%, range: 1.3–12.8%) since diatoms are the most abundant group in the plankton (Alves-de-Souza et al., 2008, and references therein). The average Si_{OPAL} value is comparable to that of Flensburg Fjord, higher than at the sites in SE Alaska, and much lower than the values recorded in laminated sediments from Canada's Saanich and Effingham inlets (Table 5).

The C/N ratios and the $\delta^{13}C$ signature of surface sediments in the Chilean fjords are very variable and similar to those reported for other fjords (Table 5), where marine and terrestrial organic carbon mix, and a clear gradient from the open ocean to the fjord heads reflects the increased contribution of terrestrial organic matter.

6. Concluding remarks

We aimed at describing a general latitudinal pattern of productivity and its imprint in the sediments of the Chilean Patagonian fjords region between 41°S and 55°S. Based on water column properties (primary production, nutrients) and surface sediment characteristics (biogenic opal, organic carbon, molar C/N, bulk sedimentary $\delta^{13}C_{org}$), we grouped the study area into four main zones: the Inner Sea of Chiloé and Northern, Central, and Southern Patagonia. A clear north–south decreasing trend in spring–summer primary production emerged (highest in the Inner Sea of Chiloé and in Northern Patagonia). Biogenic opal contents in the surface sediments mimicked this overall latitudinal pattern in primary production and were directly related to water column silicic acid concentrations. Thus, biogenic opal may be considered to be a suitable proxy for reconstructing climate-induced productivity changes during the Holocene. The higher

C/N values and the more negative carbon isotopic signal reflected an important influence from the continent, especially at the head of the fjords.

The surface silicate:nitrogen ratio ranged from >1 in the fjords of the Inner Sea of Chiloé and Northern and Central Patagonia to ~ 1 in Southern Patagonia, suggesting that a nitrate-deficiency may be responsible for the spring bloom shutdown. Experimental studies are required to establish the surface water nutrients (nitrate, silicic acid) that favor the occurrence of key phytoplankton species in the Patagonian fjords and channels.

Finally, significant reductions in the hydrological regimes of Patagonian rivers have already taken place (Lara et al., 2008) and the rapid increment of anthropogenic activity in the Chilean Patagonia may lead to changes in the fjord's nutrient inputs, primary production, key species, and the magnitude of the particulate organic carbon exported to the sediments.

Acknowledgements

This work was funded by the Center for Oceanographic Research in the eastern South Pacific (COPAS) of the University of Concepcion through the FONDAP (Project no. 150100007) and Base Financing programs (Project no. PFB-31/2007 COPAS Sur-Austral). Financial support for primary productivity data from FONDECYT Grants 1050487, 1080187, and 1070713, and FIP Grant 2007-21 is acknowledged. Funding for geochemical measurements on some PACHIDERME cores was provided by FONDECYT Grant 3085045. We are grateful to our colleagues S. Bertrand, M. Caniupán, N. Harada, R. Kilian, and P. Muñoz, who provided unpublished sediment information. We sincerely thank our personnel – Alejandro Avila, Rodrigo Castro, and Victor Acuña – for field and laboratory work. We also acknowledge the National Oceanographic Committee (CONA) for supporting our research during the CIMAR Program scientific cruises and the crews of the *AGOR Vidal Gormáz*, RV *Marion Dufresne*, RVIB *Nathaniel Palmer*, and RV *Mirai* for sampling onboard. We appreciate reviews by P. Meyers and D. Winkelmann whose corrections and suggestions helped to improve this final version. We are especially indebted to D. Winkelmann and R. Schlitzer for the high resolution maps of the Chilean Patagonia coastline and for encouraging us to use the ODV software to visualize the data. We thank Eduardo Tejos for helping with the construction of Fig. 6.

References

Abarzúa, A.M., Villagrán, C., Moreno, P.I., 2004. Deglacial and postglacial climate history in east-central Isla Grande de Chiloé, southern Chile (43° S). Quaternary Res. 62, 49–59.

Acha, E.M., Mianzan, H.W., Guerrero, R., Favero, M., Bava, J., 2004. Marine fronts at the continental shelves of austral South America: physical and ecological processes. J. Mar. Syst. 44 (1–2), 83–105.

Alves-de-Souza, C., González, M.T., Iriarte, J.L., 2008. Functional groups in marine phytoplankton assemblages dominated by diatoms in fjords of southern Chile. J. Plankton Res. 30 (11), 1233–1243.

Archer, S.D., Verity, P.G., Stefels, J., 2000. Impact of microzooplankton on the progression and fate of the spring bloom in fjords of northern Norway. Aquat. Microb. Ecol. 22, 27–41.

Ariztegui, D., Bösch, P., Davaud, E., 2007. Dominant ENSO frequencies during the Little Ice Age in Northern Patagonia: the varved record of proglacial Lago Frías, Argentina. Quaternary Int. 161, 46–55.

Avaria, S., Jorquera, L., Muñoz, P., Vera, P., 1999. Distribución de microfitoplancton marino en la zona de aguas interiores comprendida entre el golfo de Penas y el estrecho de Magallanes, Chile, en la primavera de 1996 (Crucero Cimar-Fiordo 2). Cienc. Tecnol. Mar. 22, 81–110.

Baeza, O., 2005. Lake and fjord sediments as Late Glacial to Holocene environmental and climate archives of the Southernmost Andes at 53°S, Chile. Ph.D. Thesis, University Trier, Germany, 278 pp.

Borgel, R., 1970. Geomorfología de las regiones australes de Chile. Rev. Geol. Chile 21, 135–140.

Calvert, S.E., Pedersen, T.F., Karlin, R.E., 2001. Geochemical and isotopic evidence for post-glacial palaeoceanographic changes in Saanich Inlet, British Columbia. Mar. Geol. 174, 287–305.

Dávila, P., Figueroa, D., Müller, E., 2002. Freshwater input into the coastal ocean and its relation with the salinity distribution off austral Chile (35°–55°S). Cont. Shelf Res. 22, 521–534.

Erga, S.R., 1989. Ecological studies on the phytoplankton of Boknafjorden, western Norway. II. Environmental control of photosynthesis. J. Plankton Res. 11 (4), 785–812.

Erga, S.R., Heimdal, B.R., 1984. Ecological studies on the phytoplankton of Korsfjorden, western Norway. The dynamics of a spring bloom seen in relation to hydrographical conditions and light regime. J. Plankton Res. 6 (1), 67–90.

Fabiano, M., Povero, P., Danovaro, R., Misic, C., 1999. Particulate organic matter composition in a semi-enclosed Periantarctic system: the Straits of Magellan. Sci. Mar. 63 (1), 89–98.

Fernández, H.N., Troncoso, P.C., 1984. Hidrografía. Geografía de Chile, Tomo VIII, Instituto Geográfico Militar de Chile, 320 pp.

González, H.E., Calderón, M.J., Castro, L., Clément, A., Cuevas, L.A., Danieri, G., Iriarte, J.L., Lizárraga, L., Martínez, R., Menschel, E., Silva, N., Carrasco, C., Valenzuela, C., Vargas, C.A., Molinet, C., 2010. Primary production and its fate in the pelagic food web of the Reloncaví Fjord and plankton dynamics of the Interior Sea of Chiloé, Northern Patagonia. Chile. Mar. Ecol. Prog. Ser. 402, 13–30.

Grundle, D.S., Timothy, D.A., Varela, D.E., 2009. Variations of phytoplankton productivity and biomass over an annual cycle in Saanich Inlet, a British Columbia fjord. Cont. Shelf Res. 29 (19), 2257–2269.

Gustafsson, M., Nordberg, K., 2000. Living (stained) benthic foraminifera and their response to the seasonal hydrographic cycle, periodic hypoxia and to primary production in Havstens fjord on the Swedish West Coast. Estuar. Coast. Shelf Sci. 51, 743–761.

Hay, M.B., Calvert, S.E., Pienitz, R., Dallimore, A., Thomson, R.E., Baumgartner, T.R., 2009. Geochemical and diatom signature of bottom water renewal events in Effingham Inlet, British Columbia (Canada). Mar. Geol. 262, 50–61.

Iriarte, J.L., Uribe, J.C., Valladares, C., 1993. Biomass of size-fractionated phytoplankton during the spring–summer season in Southern Chile. Bot. Mar. 36, 443–450.

Iriarte, J.L., Kush, A., Osses, J., Ruiz, M., 2001. Phytoplankton biomass in the sub-Antarctic area of the Straits of Magellan (53°S), Chile during spring–summer 1997/1998. Polar Biol. 24, 154–162.

Iriarte, J.L., González, H.E., Liu, K.K., Rivas, C., Valenzuela, C., 2007. Spatial and temporal variability of chlorophyll and primary productivity in surface waters of southern Chile (41.5–43°S). Estuar. Coast. Shelf Sci. 74, 471–480.

Kerr, A., Sudgen, D., 1994. The sensitivity of the South Chilean Snowline to climatic change. Clim. Change 28, 255–272.

Lara, A., Villalba, R., Urrutia, R., 2008. A 400-year tree-ring record of the Puelo River summer–fall streamflow in the Valdivian Rainforest eco-region, Chile. Clim. Change 86, 331–356.

Lindahl, O., Belgrano, A., Davidsson, L., Hernroth, B., 1998. Primary production, climatic oscillations, and physico-chemical process: the Gullmar fjord time-series data set (1985–1996). J. Mar. Sci. 55, 723–729.

Lliboutry, L., 1998. Glaciers of Chile and Argentina. In: Williams, R.S., Ferrigno, J.G. (Eds.), Satellite Image Atlas of Glaciers of the World, United States Geological Survey Professional Paper 1386-I, pp. I109–I206.

Magazzù, G., Panella, S., Decembrini, F., 1996. Seasonal variability of fractionated phytoplankton, biomass and primary production in the Straits of Magellan. J. Mar. Syst. 9, 249–267.

McQuoid, M.R., Nordberg, K., 2003. Environmental influence on the diatom and silicoflagellate assemblages in Koljö fjord (Sweden) over the last two centuries. Estuaries 26, 927–937.

Meyers, P.A., 1994. Preservation of elemental and isotopic source identification of sedimentary organic matter. Chem. Geol. 114, 289–302.

Meyers, P.A., 1997. Organic geochemical proxies of paleoceanographic, paleolimnologic, and paleoclimatic processes. Org. Geochem. 27, 213–250.

Miller, A., 1976. The climate of Chile. In: Schwerdtfeger, W. (Ed.), World Survey of Climatology, vol. 12. Elsevier, Amsterdam, pp. 113–145.

Mohtadi, M., Romero, O.E., Kaiser, J., Hebbeln, D., 2007. Cooling of the southern high latitudes during the Medieval Period and its effect on ENSO. Quaternary Sci. Rev. 26, 1055–1066.

Montecino, V., Pizarro, G., 2008. Primary productivity, biomass, and phytoplankton size in the austral Chilean channels and fjords: spring–summer patterns. In: Silva, N., Palma, S. (Eds.), Progress in the Oceanographic Knowledge of Chilean Interior Water, from Puerto Montt to Cape Horn. Comité Oceanográfico Nacional-Pontificia Universidad Católica de Valparaíso, pp. 93–97.

Montecino, V., Paredes, M.A., Vargas, C., Uribe, P., Giglio, S., Manley, M., Pizarro, G., 2004. Características bio-ópticas asociadas con productividad biológica en la Región de Aysén: absorción in vivo y abundancia de las fracciones de tamaños del fitoplancton en agosto y noviembre 2003. Resúmenes del crucero CIMAR 9 Fiordos. Inform. Prelimin., 89–101.

Mortlock, R., Froelich, P., 1989. A simple method for the rapid determination of biogenic opal in pelagic marine sediments. Deep-Sea Res. 36, 1415–1426.

Müller, A., 2001. Geochemical expressions of anoxic conditions in Nordåsvannet, a land-locked fjord in Western Norway. Appl. Geochem. 16, 363–374.

Muñoz, P., Lange, C.B., Gutierrez, D., Hebbeln, D., Salamanca, M.A., Dezileau, L., Reyss, J.L., Benninger, L.K., 2004. Recent sedimentation and mass accumulation rates based on ^{210}Pb along the Peru–Chile continental margin. Deep-Sea Res. Pt. II 51 (20–21), 2523–2541.

New, M., Lister, D., Hulme, M., Makin, I., 2002. A high-resolution data set of surface climate over global land areas. Clim. Res. 21, 1–25.

Nikulina, A., Dullo, W.-C., 2009. Eutrophication and heavy metal pollution in the Flensburg Fjord: a reassessment after 30 years. Mar. Pollut. Bull. 58, 905–915.

Nikulina, A., Polovodova, I., Schönfeld, J., 2008. Foraminiferal response to environmental changes in Kiel Fjord, SW Baltic Sea. eEarth 3, 37–49.

Palma, S., 2008. Zooplankton distribution and abundance in the austral Chilean channels and fjords. In: Silva, N., Palma, S. (Eds.), Progress in the Oceanographic Knowledge of Chilean Interior Waters, from Puerto Montt to Cape Horn. Comité Oceanográfico Nacional-Pontificia Universidad Católica de Valparaíso, Valparaíso, pp. 107–113.

Palma, S., Silva, N., 2004. Distribution of siphonophores, chaetognaths, euphausiids and oceanographic conditions in the fjords and channels of southern Chile. Deep-Sea Res. Pt. II 51, 513–535.

Paredes, M.A., Montecino, V., this issue. Size diversity as an expression of phytoplankton structure and the identification of its patterns on the scale of fjords and channels. Cont. Shelf Res.

Pickard, G.L., 1971. Some physical oceanographic features of Inlets of Chile. J. Fish. Res. Board Can. 28, 1077–1106.

Pinto, L., Bonert, C., 2005. Origen y distribución espacial de hidrocarburos alifáticos en sedimentos de Seno Aysén y Canal Moraleda, Chile Austral. Cienc. Tecnol.Mar. 28 (1), 35–44.

Pizarro, G., Iriarte, J.L., Montecino, V., Blanco, J.L., Guzmán, L., 2000. Distribución de la biomasa fitoplanctónica y productividad primaria máxima de fiordos y canales australes (47–50°S) en octubre de 1996. Comité Oceanogr. Nacional 23, 25–48.

Pizarro, G., Montecino, V., Guzmán, L., Muñoz, V., Chacón, V., Pacheco, H., Frangópulos, M., Retamal, L., Alarcón, C., 2005. Patrones locales recurrentes del fitoplancton en fiordos y canales australes (46°-56° S) en primavera y verano. Cienc. Tecnol. Mar. 28 (2), 63–83.

Rabassa, J., 2008. Late Cenozoic Glaciations in Patagonia and Tierra del Fuego. In: Rabassa, J. (Ed.), The Late Cenozoic of Patagonia and Tierra del Fuego. Developments in Quaternary Science 11 series Elsevier, Amsterdam, pp. 151–204.

Rebolledo, L., 2007. Variabilidad temporal en la productividad durante los últimos ~1800 años en los fiordos chilenos de Patagonia Norte (44–46°S). Ph.D. Thesis, Universidad de Concepción, 162 pp.

Rebolledo, L., Lange, C.B., Figueroa, D., Pantoja, S., Muñoz, P., Castro, R., 2005. 20th century fluctuations in the abundance of siliceous microorganisms preserved in the sediments of the Puyuhuapi Channel (44°S), Chile. Rev. Chil. Hist. Nat. 78 (3), 469–488.

Rebolledo, L., Sepúlveda, J., Lange, C.B., Pantoja, S., Bertrand, S., Hughen, K., Figueroa, D., 2008. Late Holocene marine productivity changes in Northern Patagonia-Chile inferred from a multi-proxy analysis of Jacaf channel sediments. Estuar. Coast. Shelf Sci. 80, 314–322.

Rebolledo, L., González, H.E., Muñoz, P., Iriarte, J., Lange, C.B., Pantoja, S., Salamanca, M., this issue. Siliceous productivity changes in Gulf of Ancud sediments (42°S, 72°W), southern Chile, over the last ~150 years. Cont. Shelf Res.

Rivera, A., Acuña, C., Casassa, G., Bown, F., 2002. Use of remote sensing and field data to estimate the contribution of Chilean glaciers to the sea level rise. Ann. Glaciol. 34, 367–372.

Rojas, N., 2002. Distribución de materia orgánica, carbono y nitrógeno, y diagénesis temprana en sedimentos de la zona de canales australes entre los golfos Corcovado y Elefantes, Chile. Undergraduate Thesis, Universidad Católica de Valparaíso, Valparaíso, Chile, 76 pp.

Rojas, N., Silva, N., 2005. Early diagenesis and vertical distribution of organic carbon and total nitrogen in recent sediments of the Chilean fjords: Boca del Guafo (43°47' S) to canal Pulluche (45° 49' S). Invest. Mar. 33 (2), 183–194.

Saggiomo, V., Goffart, A., Carrada, G.C., Hecq, J.H., 1994. Spatial patterns of phytoplanktonic pigments and primary production in a semi-enclosed periantarctic ecosystem: the Straits of Magellan. J. Mar. Syst. 5, 119–142.

Salamanca, M.A., Jara, B., 2003. Distribución y acumulación de plomo (Pb y ^{210}Pb) en sedimentos de los fiordos de la XI región, Chile. Cienc. Tecnol. Mar. 26, 61–71.

Schneider, C., Glaser, M., Kilian, R., Santana, A., Butorovic, N., 2003. Weather observations across the southern Andes at 53°S. Phys. Geog. 24 (2), 97–119.

Sepúlveda, J., 2005. Aporte de material terrígeno en fiordos de Patagonia del Norte: Evidencia geoquímica en sedimentos recientes y del Holoceno tardío. M.Sc. Thesis, Universidad de Concepción, Chile, 143 pp.

Sepúlveda, J., Pantoja, S., Hughen, K., Lange, C., González, F., Muñoz, P., Rebolledo, L., Castro, R., Contreras, S., Ávila, A., Rossel, P., Lorca, G., Salamanca, M., Silva, N., 2005. Fluctuations in export productivity over the last century from sediments of a southern Chilean fjord (44°S). Estuar. Coast. Shelf Sci. 65, 587–600.

Sepúlveda, J., Pantoja, S., Hughen, K.A., Bertrand, S., Figueroa, D., León, T., Drenzek, N.J., Lange, C., 2009. Late Holocene sea-surface temperature and precipitation variability in northern Patagonia, Chile (Jacaf Fjord, 44°S). Quaternary Res. 72 (3), 400–409.

Sepúlveda, J., Pantoja, S., Hughen, K. A., this issue. Sources and distribution of organic matter in northern Patagonian fjords, Chile (~44–47°S): a multi-tracer approach for carbon cycling assessment. Cont. Shelf Res.

Sievers, H.A., Silva, N., 2008. Water masses and circulation in austral Chilean channels and fjords. In: Silva, N., Palma, S. (Eds.), Progress in the Oceanographic Knowledge of Chilean Interior Water, from Puerto Montt to Cape Horn. Comité Oceanográfico Nacional-Pontificia Universidad Católica de Valparaíso, pp. 53–58.

Silva, N., 2008. Physical and chemical characteristics of the surface sediments in the austral Chilean channels and fjords. In: Silva, N., Palma, S. (Eds.), Progress in the Oceanographic Knowledge of Chilean Interior Waters, from Puerto Montt to Cape Horn. Comité Oceanográfico Nacional-Pontificia Universidad Católica de Valparaíso, Valparaíso, pp. 69–75.

Silva, N., Calvete, C., 2002. Características oceanográficas físicas y químicas de canales australes chilenos entre el golfo Penas y el estrecho de Magallanes (Crucero CIMAR Fiordo 2). Cienc. Tecnol. Mar. 25 (1), 23–88.

Silva, N., Neshyba, S., 1979. On the southernmost extension of the Peru–Chile Undercurrent. Deep-Sea Res. 26A, 1378–1393.

Silva, N., Palma, S., 2008. The CIMAR Program in the austral Chilean channels and fjords. In: Silva, N., Palma, S. (Eds.), Progress in the Oceanographic Knowledge of Chilean Interior waters, from Puerto Montt to Cape Horn. Comité Oceanográfico Nacional-Pontificia Universidad Católica de Valparaíso, Valparaíso, pp. 11–15.

Silva, N., Prego, R., 2002. Carbon and nitrogen spatial segregation and stoichiometry in the surface sediments of southern Chilean inlets (41–56°S). Estuar. Coast. Shelf Sci. 55, 763–775.

Silva, N., Sievers, H., Prado, R., 1995. Características oceanográficas y una proposición de circulación, para algunos canales australes de Chile entre 41° 20' y 46°40' S. Rev. Biol. Mar. 30 (2), 207–254.

Silva, N., Calvete, C., Sievers, H.A., 1997. Características oceanográficas físicas y químicas de canales australes chilenos entre Puerto Montt y laguna San Rafael (Crucero CIMAR-Fiordo 1). Cienc. Tecnol. Mar. 20, 23–106.

Silva, N., Calvete, C., Sievers, H.A., 1998. Masas de agua y circulación general para algunos canales australes entre Puerto Montt y Laguna San Rafael, Chile (Crucero Cimar-Fiordo 1). Cienc. Tecnol. Mar. 21, 17–48.

Silva, N., De Vidts, V., Sepúlveda, J., 2001. Materia orgánica, C y N y su distribución y estequiometría en sedimentos superficiales de la región central de los fiordos y canales australes de Chile (Crucero CIMAR Fiordo 2). Cienc. Tecnol. Mar. 24, 23–40.

Silva, N., Haro, J., Prego, R., 2009. Metals background and enrichment in the Chiloé Interior Sea sediments (Chile). Is there any segregation between fjords, channels and sounds? Estuar. Coast. Shelf Sci. 82 469–476.

Silva, N., Vargas, C.A., Prego, R., this issue. Land–ocean distribution of allochthonous organic matter in the surface sediments of the Chiloé and Aysén Interior Seas (Chilean Northern Patagonia). Cont. Shelf Res..

Steemann-Nielsen, E., 1952. The use of radiocarbon (^{14}C) for measuring organic production in the sea. J. Conseil Permanent Inte. l' Explo. Mer. 18, 117–140.

St-Onge, G., Hillaire-Marcel, G., 2001. Isotopic constraints of sedimentary inputs and organic carbon burial rates in the Saguenay fjord, Quebec. Mar. Geol. 176, 1–22.

Strub, P.T., Mesias, J., Montecino, V., Rutllant, J., Salinas, S., 1998. Coastal ocean circulation off Western South America Coastal segment (6, E). In: Robinson, A.R., Brink, K.H. (Eds.), The Sea, vol. 11. John Wiley & Sons, Inc., New York, pp. 273–313.

Torres, R., Frangópulos, M., Hamamé, M., Montecino, V., Maureira, C., Pizarro, G., Reid, B., this issue. Nitrate to silicate ratio variability and the composition of micro-phytoplankton blooms in the inner-fjord of Seno Ballena (Strait of Magellan, 54°S). Cont. Shelf Res.

Torres, R., Pantoja, S., Harada, N., Gonzalez, H., Daneri, G., Frangópulos, M.,. Rutllant, J., Duarte, C., Rúiz-Halpern, S., Mayol, E., Fukasawa, M. Air–sea CO_2 fluxes along the coast of Chile: from CO_2 outgassing in central–northern upwelling waters to CO_2 sequestering in southern Patagonian fjords. J. Geophys. Res, submitted for publication.

Valdenegro, A., Silva, N., 2003. Caracterización física y química de la zona de canales y fiordos australes de Chile entre el Estrecho de Magallanes y Cabo de Hornos (CIMAR 3 Fiordos). Cienc. Tecnol. Mar. 26 (2), 19–60.

Vargas, C.A., Martinez, R.A., San Martin, V., Aguayo, M., Silva, N., Torres, R., this issue. Allochthonous subsides of organic matter across a lake–river–fjord landscape in the Chilean Patagonia: implication for marine plankton food webs. Cont. Shelf Res.

Velinsky, D.J., Fogel, M.L., 1999. Cycling of dissolved and particulate nitrogen and carbon in the Framvaren Fjord, Norway: stable isotopic variations. Mar. Chem. 67, 161–180.

Villagrán, C., 1988. Expansion of magellanic moorland during the late pleistocene: palynological evidence from Northern Isla de Chiloe, Chile. Quaternary Res. 30, 304–314.

Walinsky, S.E., Prahl, F.G., Mix, A.C., Finney, B.P., Jaeger, J.M., Rosen, G.P., 2009. Distribution and composition of organic matter in surface sediments of coastal Southeast Alaska. Cont. Shelf Res. 29, 1565–1579.

Winkelmann, D., Knies, J., 2005. Recent distribution and accumulation of organic carbon on the continental margin west off Spitsbergen. Geochem. Geophys. Geosyst., 6. doi:10.1029/2005GC000916.